# Prostate Cancers

**5**

L. Allainmat, A. Baskin, T. De Perrot, M. Eiber,
M. Souvatzoglou, and J.-P. Vallée

## Contents

L. Allainmat (✉) • A. Baskin
Department of Imaging, Division of Nuclear Medicine
and Molecular Imaging, Geneva University Hospital,
Geneva, Switzerland
e-mail: laurent.allainmat@hcuge.ch

T. De Perrot • J.-P. Vallée
Department of Imaging, Division of Radiology,
Geneva University Hospital,
Geneva, Switzerland

M. Eiber
Department of Radiology, Klinikum Rechts der Isar,
Technische Universität München, Munich, Germany

M. Souvatzoglou
Department of Nuclear Medicine, Klinikum Rechts der Isar,
Technische Universität München, Munich, Germany

## Prostate Cancers

Prostate cancer is biologically and clinically a heterogeneous disease that makes imaging evaluation challenging because different stages of prostate cancer are managed with different treatment modalities.

The role of imaging in prostate cancer includes diagnosis, localization and characterization of the primary tumor, determination of extracapsular spread, guidance and evaluation of local therapy, staging of locoregional lymph nodes, detection of locally recurrent and metastatic disease in biochemical relapse, and planning of radiation treatment [1].

The most commonly used imaging modalities for diagnosing and staging prostate cancer are transrectal ultrasound, dedicated MRI and bone scintigraphy. New developments in radiotracers such as radiolabelled Choline and Acetate have brought a new scope of applications of PET in the diagnosis and follow-up of prostate cancers.

Prostate magnetic resonance imaging (MRI) plays an important role in the determination of tumor localization, characteristics, and extent [2]. Multiparametric MRI complementes T2W images with diffusion-weighted imaging, dynamic contrast-enhanced (DCE) imaging, and MR spectroscopy imaging (MRSI) to improve diagnostic accuracy. Multiparametric MRI still remains imperfect, with sensitivities and specificities ranging from 22–85 % to 50–99 % [3]. In particular morphologic lymph node assessment with MRI is limited.

PET has emerged as a promising imaging tool for prostate cancer. However, ^{18}F-FDG, has limited sensitivity for prostate cancer [4, 5] due to low glucose consumption in early prostate cancer [6, 7]. ^{18}F-choline and ^{11}C-Choline has shown promise in the detection of prostate cancer, especially in the setting of recurrent and metastatic disease [8–18].

Hybrid PET/MRI scanners introduced recently into clinical practice [19, 20] combine the advantages of both modalities with reduced ionizing radiation, shorter acquisition times and better diagnostic accuracy especially in recurrences and localized prostate cancers.

## Prostate Focal Adenocarcinoma

### Clinical History

Fifty-nine-year-old patient with a primary prostate adenocarcinoma discovered through clinical examination and further confirmed by biopsy (Gleason: 4 + 3).

### Imaging Technique

PET: 10 min dynamic acquisition obtained immediately after injection of 240 MBq of F-18 Fluorocholine followed by whole body scan obtained 10 min after injection and a late acquisition centered on the prostate.

MRI: a complete diagnostic MRI study was acquired in the same session including a 2D T2 Fast SE (TR/TE 4,000/120 ms – slice thickness 3 mm – 432 × 386 for the axial acquisition – FOV 22 cm) with both an endorectal coil and an external 6 array coil, and after removal of the endorectal coil, a 3D T2 fast spin echo MR sequence (3D VISTA) (TR/TE 2,000/243 ms, matrix 392 × 448/×25, FOV 390 mm and slice thickness 1 mm), a diffusion SE EPI sequence (TR/TE 3,644/66 ms – slice thickness 3 mm – FOV 200 mm – matrix 88/×9, 4 b values 0, 500, 1,000, 1,500 s/mm$^2$).

### Findings

PET images show focal tracer uptake (SUV max 12.8) in the antero-apical area of the central zone predominantly on the right side matching the first lesion identified on MRI but not the second MRI lesion in the left peripheral zone.

MRI images showed two focal abnormalities: one in the right antero-apical area of the central zone with a hypointensity on the T2 images, and decreased diffusion (ADC at 800), and a second lesion in the left peripheral zone of the apex with decreased T2 signal and decreased diffusion (ADC at 900) adjacent to the central zone.

The histology performed after radical prostatectomy demonstrated an adenocarcinoma in the antero-apical area of the central zone and prostatic intraepithelial neoplasia in the left peripheral zone.

### Teaching Points

Correlation between anatomical, functional and metabolic images: intra-epithelial neoplasia was a false positive on the T2 and diffusion MRI but not on the PET images.
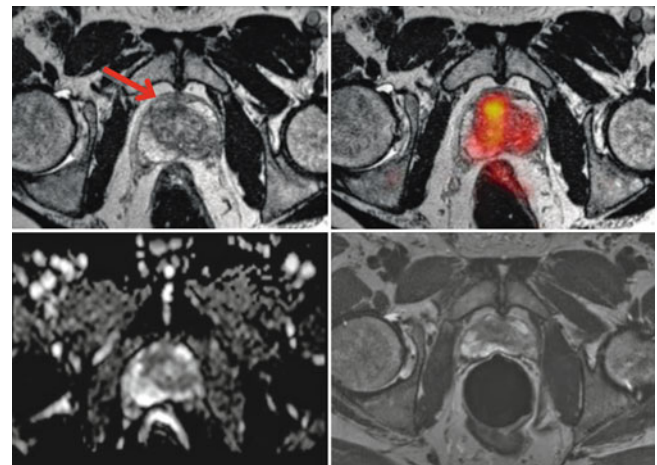


**Fig. 5.2** Fused PET/MR images (*upper row*) showing the localization of a focal antero-apical lesion of decreased T2 MR signal (3D VISTA) (*red arrow*) and positive FDG uptake. *Lower row* shows additional diagnostic MR sequences with diffusion weighted images (DWI SSH) and a T2 TSE images obtained with endorectal coil. A prostatic intra-epithelial neoplasia in the left peripheral zone showed a decreased T2 and diffusion signal but no abnormality on the PET



**Fig. 5.1** 3D MIP images of whole body PET showing focal uptake (*arrow*) in the prostate area but no other signs of dissemination or metastases
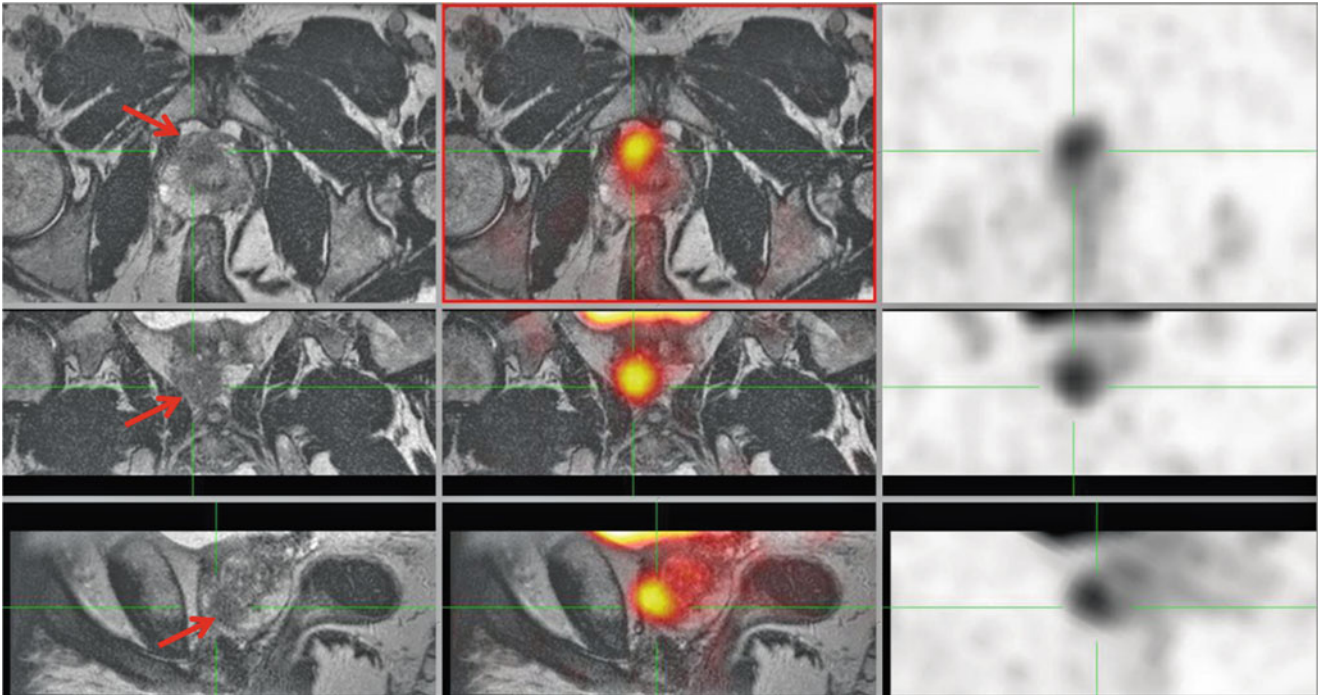
**Fig. 5.3** Fused PET/MR images showing the localization (*red arrow*) of a focal antero-apical lesion of decreased T2 MR signal on a 3D VISTA and positive radiotracer uptake
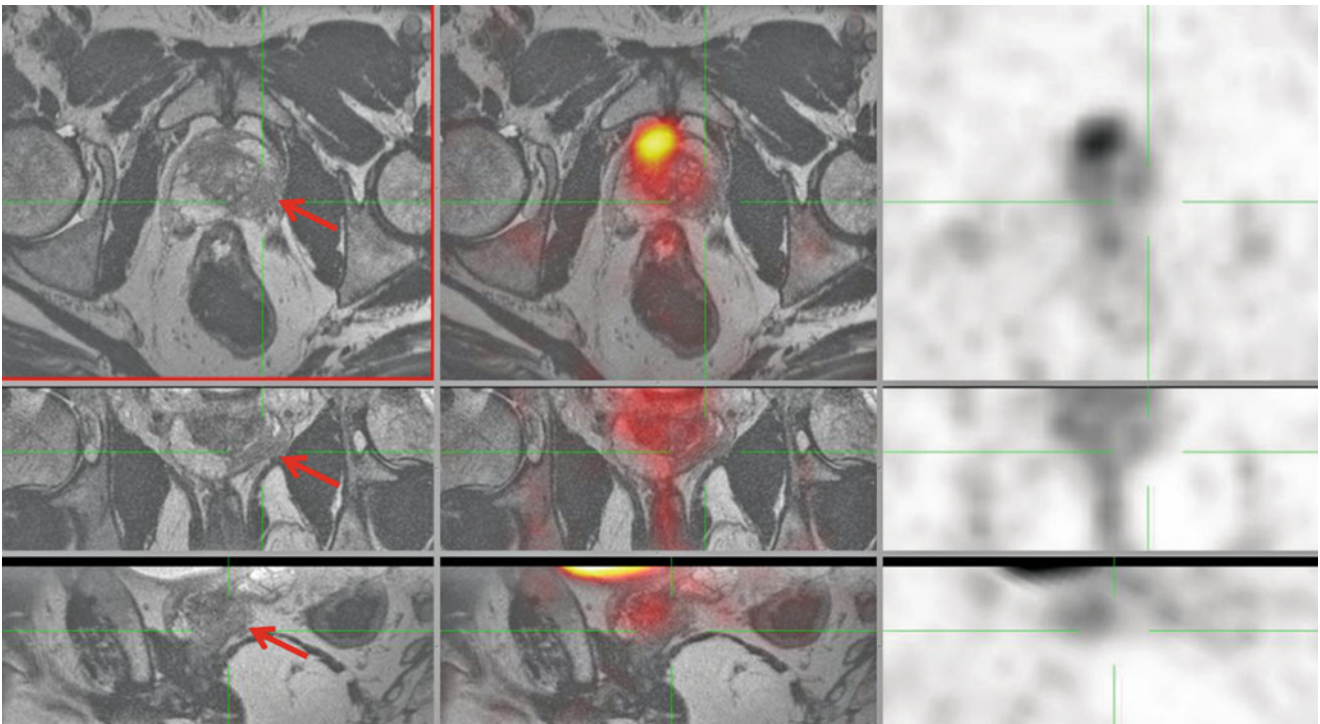


**Fig. 5.4** Fused PET/MR images showing a lesion with decreased T2 MR signal (*red arrow*) on a 3D VISTA and no radiotracer uptake

## Multifocal Prostate Cancer

### Clinical History

Staging of a prostatic adenocarcinoma with a Gleason score 3+4.

### Imaging Technique

PET: 10 min dynamic acquisition obtained immediately after injection of 317 MBq of F-18 Fluorocholine followed by whole body scan obtained 10 min after injection and a late acquisition centered on the prostate.

MRI: a complete diagnostic MRI study was acquired in the same session including a 2D T2 Fast SE (TR/TE 4,000/120 ms – slice thickness 3 mm – 432×386 for the axial acquisition – FOV 22 cm) with both an endorectal coil and an external 6 array coil, and after removal of the endorectal coil, a 3D T2 fast spin echo MR sequence (3D VISTA) (TR/TE 2,000/243 ms, matrix 392×448/×25, FOV 390 mm and slice thickness 1 mm), a diffusion SE EPI sequence (TR/TE 3,644/66 ms – slice thickness 3 mm – FOV 200 mm – matrix 88/×9, 4 b values 0, 500, 1,000, 1,500 s/mm²) and a multiframe 3D T1 Fat Saturation gradient echo MR sequence (TR/TE 6.9 – 3.4 ms – matrix 192×189 – FOV 210 mm – slice thickness 3 mm) during 5 min after Gd-chelate injection.

### Findings

The left peripheral zone at 4 o'clock in the base of the prostate showed a high tracer uptake (SUV max=4) as well as reduced T2 signal and apparent diffusion coefficient ADC and an increase wash-in on the perfusion MRI after Gd injection. In the right peripheral zone at 7 o'clock, there was also an area of T2, diffusion and perfusion abnormalities on MRI but only a weak tracer uptake on the PET images (SUV max=2.3). Note also a moderate hypermetabolism in the central zone associated with an hyperperfusion and a mild restriction of the apparent coefficient of diffusion but no T2 abnormality in the right central zone.

Histology confirmed an adenocarcinoma in both the left and right peripheral zone.

### Teaching Points

A low tracer uptake of a lesion does not exclude a prostatic cancer. The normal central gland can show moderate tracer uptake by comparison to the peripheral zone.
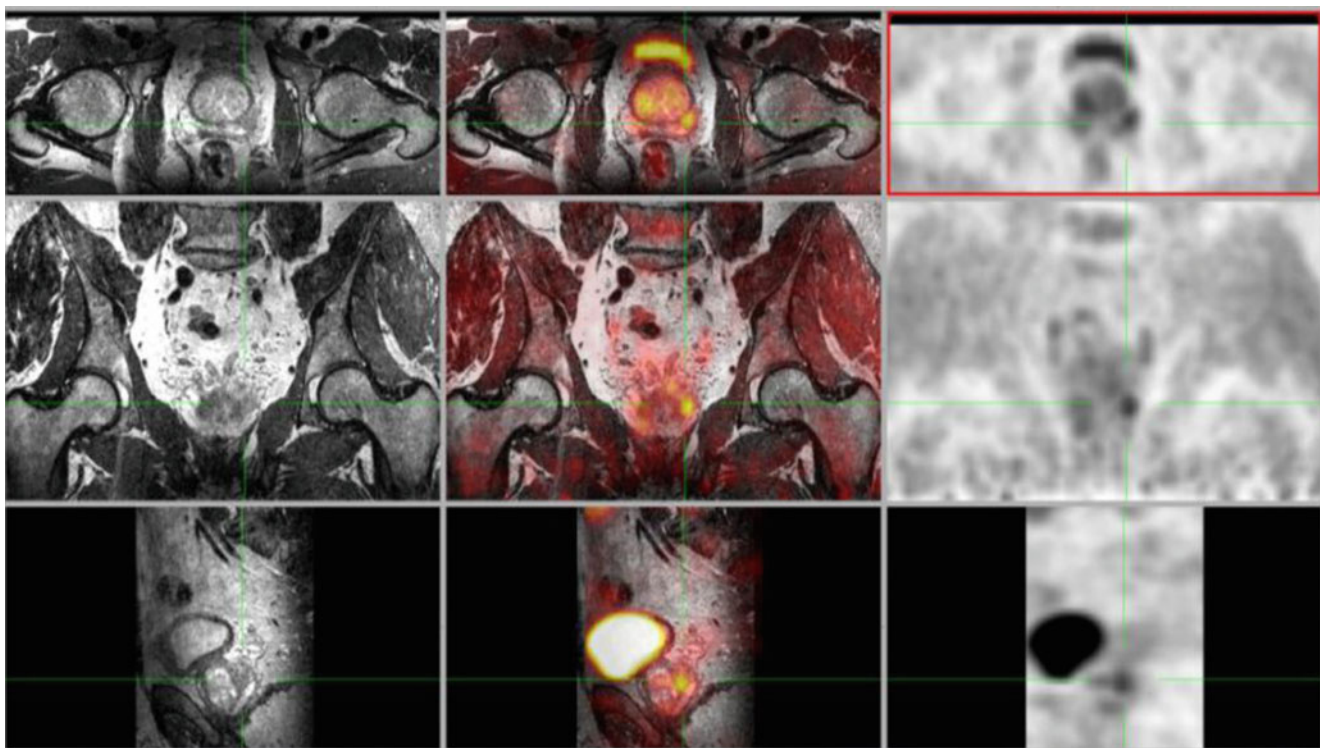


**Fig. 5.5** Fused PET/MR images showing the localization of a left peripheral zone at the base of decreased T2 MR signal on a 3D VISTA and positive radiotracer uptake. Note the absence of abnormal lymph nodes
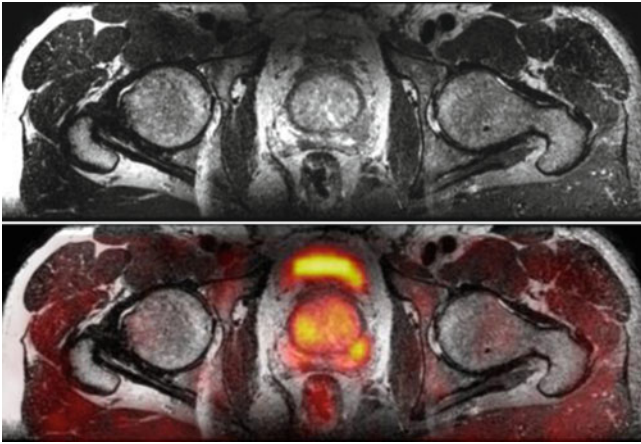
**Fig. 5.6** T2 weighted 3D VISTA axial MRI images (*upper row*) and after fusion with PET (*lower row*) showing tracer uptake in the left peripheral zone at 4 o'clock as well as a T2 hyposignal. At 7 o'clock there is also a weak tracer uptake a as well as a T2 hypointensity



**Fig. 5.8** Perfusion MRI with 3D fast GRE after Gd injection demonstrates foci of hyperperfusion in the right central zone and in the peripheral zone at 4 o'clock and 7 o'clock (*arrows*)
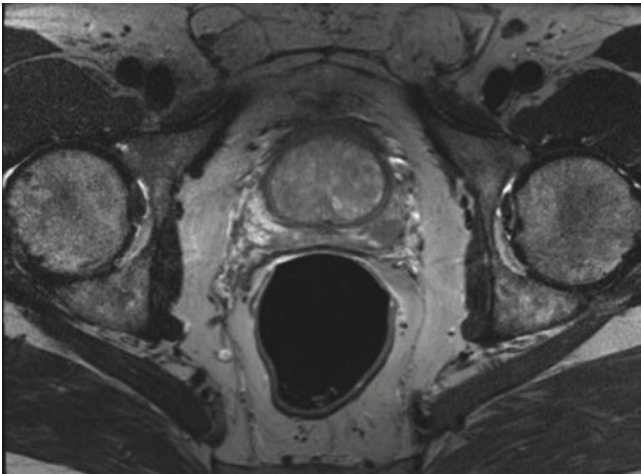


**Fig. 5.7** Hypointense T2 signal at 4 o'clock and at 7 o'clock in the peripheral zone of the prostate with a T2 FSE MR sequence and an endorectal coil
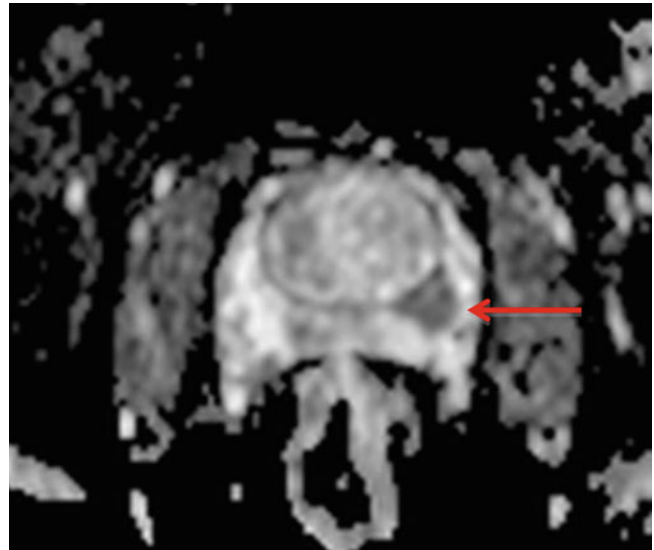


**Fig. 5.9** The diffusion MRI shows an area of strong restriction of the apparent diffusion coefficient in the left peripheral zone at 4 o'clock (*arrow*)

## Prostate Cancer with Invasion of Regional Lymph Nodes

### Clinical History

Staging of a prostatic adenocarcinoma with a Gleason score of 4+4 discovered by an increased PSA serum level (14.7 ng/ml).

### Imaging Technique

PET: 10 min dynamic acquisition obtained immediately after injection of 240.3 MBq of F-18 Fluorocholine followed by whole body scan obtained 10 min after injection and a late acquisition centered on the prostate.

MRI: a complete diagnostic MRI study was acquired in the same session including a 2D T2 Fast SE (TR/TE 4,000/120 ms – slice thickness 3 mm – $432 \times 386$ for the axial acquisition – FOV 22 cm) with both an endorectal coil and an external 6 array coil, and after removal of the endorectal coil, a 3D T2 fast spin echo MR sequence (3D VISTA) (TR/TE 2,000/243 ms, matrix $392 \times 448/\times 25$, FOV 390 mm and slice thickness 1 mm), a diffusion SE EPI sequence (TR/TE 3,644/66 ms – slice thickness 3 mm – FOV 200 mm – matrix $88/\times 9$, 4 b values 0, 500, 1,000, 1,500 s/mm$^2$) and a multi-frame 3D T1 Fat Saturation gradient echo MR sequence (TR/TE 6.9 – 3.4 ms – matrix $192 \times 189$ – FOV 210 mm – slice thickness 3 mm during 5 min after Gd-chelate injection.

### Findings

Large lesion in the right peripheral zone from 7 to 9 o'clock extending from the base to the apex with an hypointensity on the T2 MR sequences, a restriction of the apparent diffusion coefficient (ADC) and an hypervascularisation as well as an increased radiotracer uptake (SUV max = 6.8) associated to a loss of the adjacent capsule reflecting an extracapsular dissemination. In the right anterior part of the prostate, a retention cyst is also seen that is hyperintense on T2, with a high ADC and no metabolism on the PET images. In addition, both MRI and PET (SUV max = 10.4) show an abnormal right iliac lymph node. PET also detected a bone metastasis on the roof of the left acetabulum (SUV max = 4.0) that was difficult to diagnose on the T2 Fast SE MR sequences optimized for the prostate but not for bone analysis.

### Teaching Points

Good correlation between MRI and PET for the detection of the adenocarcinoma.

Extracapsular dissemination is best diagnosed by T2 2D FSE with the endorectal coil.

PET is a very efficient tool for the detection of bone metastasis due to the limited bone marrow contrast of MR sequences used for the prostate evaluation.
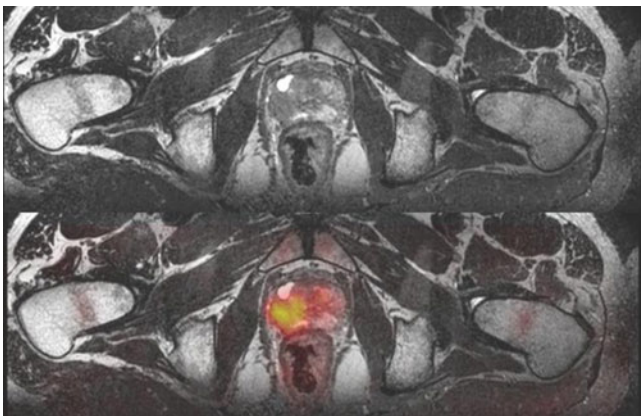


**Fig. 5.10** T2 3D vista with (*bottom*) and without (*top*) fusion with the PET data. The adenocarcinoma in the right peripheral zone is hypointense in T2 and hypermetabolic on the PET
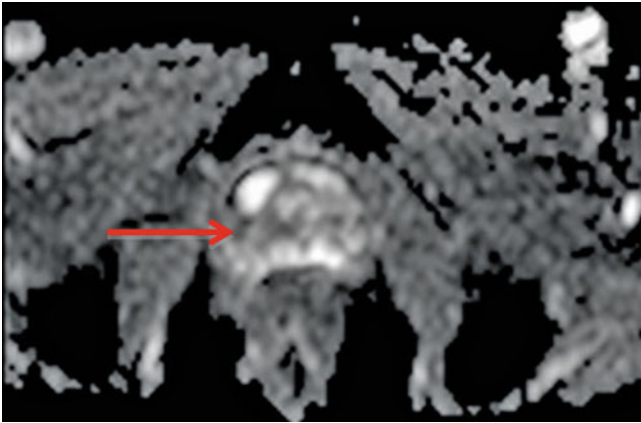
**Fig. 5.11** Diffusion weighted image. An area of restriction of the apparent coefficient of diffusion (ADC) is present in the right peripheral zone between 7 and 9 o'clock (*arrow*). Note the presence of retention cyst located anterior to this zone with a high ADC
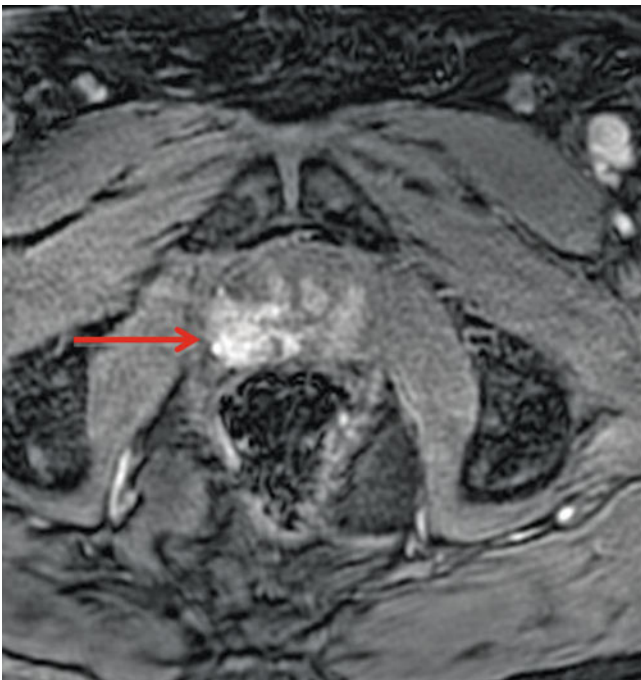


**Fig. 5.12** Dynamic thrive image sequence; the adenocarcinoma in the right peripheral zone (*arrow*) is hypervascularized on the perfusion MRI obtained after Gd injection



**Fig. 5.13** The 2D T2 FSE MR sequence acquired with an endorectal coil shows a hypointense area (*red arrow*) in the right peripheral zone with a loss of the prostatic capsule in front of the right neurovascular bundle corresponding to an extracapsular extension of the tumor
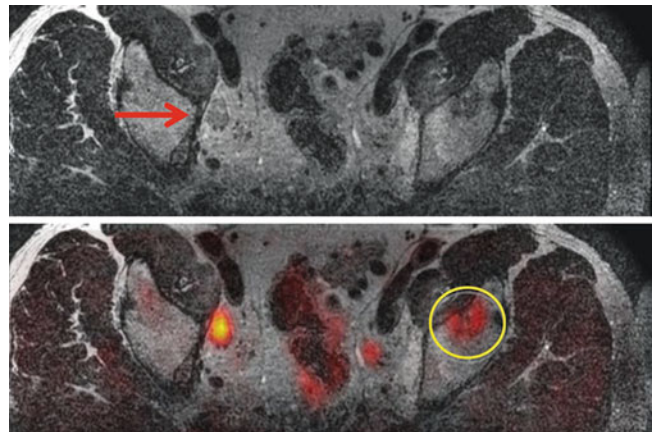


**Fig. 5.14** Fused PET/MR images showing a right iliac adenopathy on the 3D VISTA with an abnormal radiotracer uptake (*red arrow*). There is also an abnormal radiotracer uptake on the roof of the left acetabulum corresponding to a bone metastasis that is barely visible on the fast SE 3D VISTA MR sequence (*yellow circle*)

## Prostate Cancer with Capsular Invasion

### Clinical History

Staging of extension of primary prostate cancer in a 72 year old patient with a primary prostate adenocarcinoma discovered through clinical examination. Gleason (3+4). PSA at 13 µg/l.

### Imaging Technique

<u>PET</u>: 10 min dynamic acquisition obtained immediately after injection of 240 MBq of F-18 Fluorocholine followed by whole body scan obtained 10 min after injection and a late acquisition centered on the prostate.

<u>MRI</u>: a complete diagnostic MRI study was acquired in the same session including a 2D T2 Fast SE (TR/TE 4,000/120 ms – slice thickness 3 mm – 432×386 for the axial acquisition – FOV 22 cm) with both an endorectal coil and an external 6 array coil, and after removal of the endorectal coil, a 3D T2 fast spin echo MR sequence (3D VISTA) (TR/TE 2,000/243 ms, matrix 392×448/×25, FOV 390 mm and slice thickness 1 mm), a diffusion SE EPI sequence (TR/TE 3,644/66 ms – slice thickness 3 mm – FOV 200 mm – matrix 88/×9, 4 b values 0, 500, 1,000, 1,500 s/mm$^2$) and a multiframe 3D T1 Fat Saturation gradient echo MR sequence (TR/TE 6.9 – 3.4 ms – matrix 192×189 – FOV 210 mm – slice thickness 3 mm) during 5 min after Gd-chelate injection.

### Findings

PET images show focal hypermetabolic nodule (SUV max of 3) at the lower right quadrant (8 o'clock) measuring approximately 6 mm in diameter and depicted with hyposignal on T2 weighted images and hypervascular irregular shape extending beyond the external capsule.

A second lesion measuring 2.5 × 0.4 cm with hypointense signal on T2 images and focal hypermetabolism (SUVmax = 2.6) is identified in the left apical area with extension beyond the external capsule.

> ### Teaching Points
>
> This case illustrates the added value of MRI for the assessment of capsular invasion of tumoral tissue that can hardly be detected by PET images.
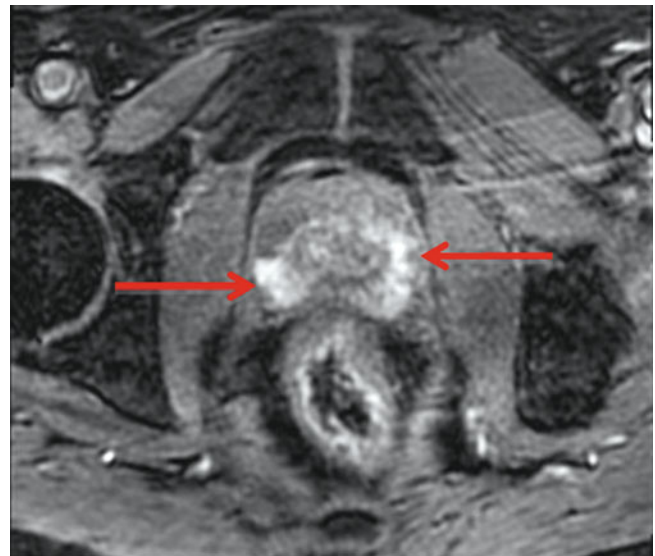


**Fig. 5.16** Perfusion weighted images (WIP DYN THRIVE NEW SENSE) showing the hypervascular nature of the lesions on both sides (*arrows*)



**Fig. 5.15** T2-PET MR (3D VISTA) fusion image showing two hypointense and hypermetabolic lesions in the right and left lobes, with heterogeneous pattern of the prostate capsule in contact with the tumor
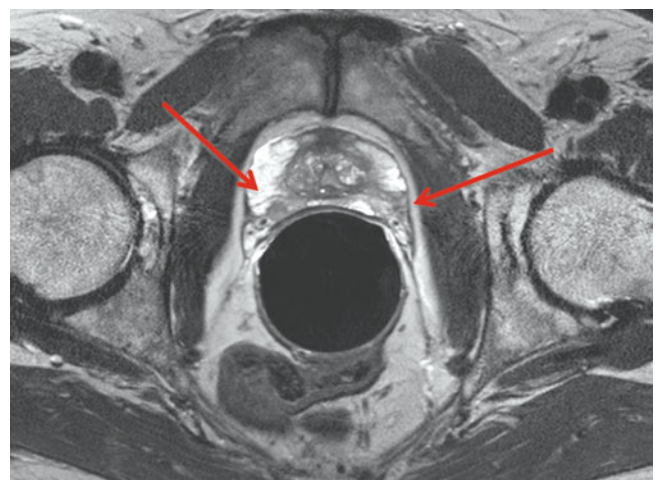


**Fig. 5.17** T2 TSE images obtained with rectal coil showing two hypointense lesions (*arrows*) more visible in this sequence
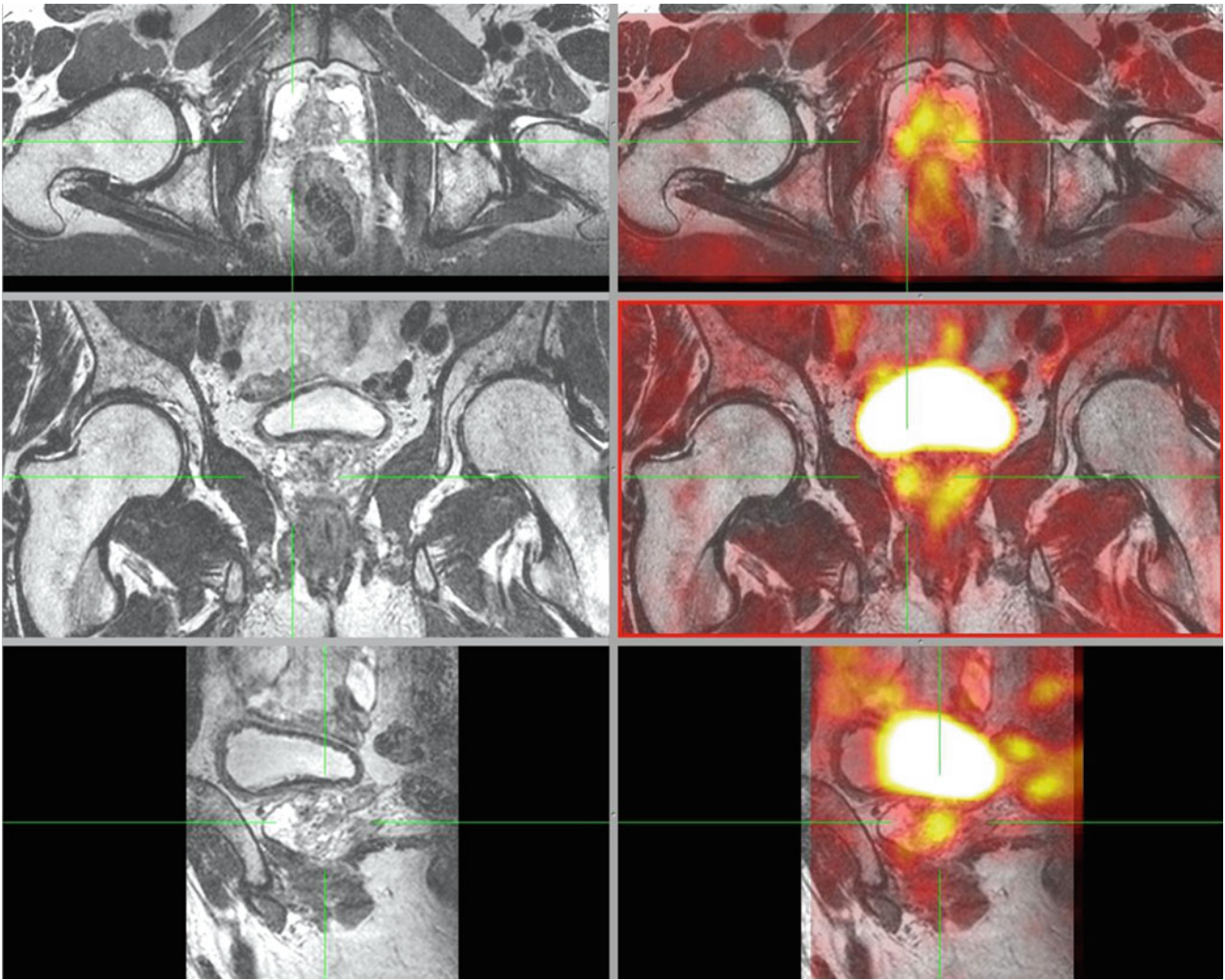
**Fig. 5.18** 3D VISTA, multiplanar image fusion centered on the most hypermetabolic lesion, showing two lesions on the right and left with heterogeneous appearance of the prostate capsule in contact with the tumor

## Prostate Cancer with Lymph Node Extension

### Clinical History

Staging of a prostatic adenocarcinoma with a Gleason score of $5+4$ and a PSA level at 13.7 µg/l.

### Imaging Technique

PET: 10 min dynamic acquisition obtained immediately after injection of 240 MBq of F-18 Fluorocholine followed by whole body scan obtained 10 min after injection and a late acquisition centered on the prostate.

MRI: a complete diagnostic MRI study was acquired in the same session including a 2D T2 Fast SE (TR/TE 4,000/120 ms – slice thickness 3 mm – 432×386 for the axial acquisition – FOV 22 cm) with both an endorectal coil and an external 6 array coil, and after removal of the endorectal coil, a 3D T2 fast spin echo MR sequence (3D VISTA) (TR/TE 2,000/243 ms, matrix 392×448/×25, FOV 390 mm and slice thickness 1 mm), a diffusion SE EPI sequence (TR/TE 3,644/66 ms – slice thickness 3 mm – FOV 200 mm – matrix 88/×9, 4 b values 0, 500, 1,000, 1,500 s/mm$^2$) and a multi-frame 3D T1 Fat Saturation gradient echo MR sequence (TR/TE 6.9 – 3.4 ms – matrix 192×189 – FOV 210 mm – slice thickness 3 mm during 5 min after Gd-chelate injection.

### Findings

Large prostatic tumor invading all the right peripheral zone with some extension on the left side with a strong hypointensity on T2 images, an hypervascularization on perfusion MRI as well as a strong restriction of the apparent diffusion coefficient (ADC). On the PET images, this lesion has a strong uptake of the radiotracer (SUV max = 9.3). In front of the right neurovascular bundle, there is a loss of the capsule reflecting extracapsular dissemination. In addition, three lymph nodes of the right iliac chain demonstrated a strong uptake of the radiotracer corresponding to metastasic adenopathies (max SUVmax from 4.6 to 8.1). On the MRI, two of these abnormal lymph nodes were infracentimetric (6 and 5 mm) and were erroneously classified as benign lymph nodes.

### Teaching Points

This case demonstrates strong correlation between MRI and PET for the tumor localization.

Advantage of MRI for identification of the transgression of the prostatic capsule.

Advantage of PET for lymph node staging.



**Fig. 5.19** T2 weighted MR image and PET/MR fusion showing the hypointense lesion on the right
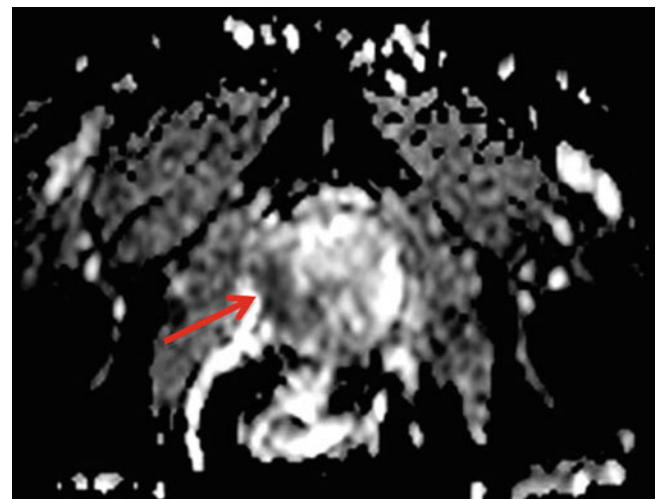


**Fig. 5.20** The apparent diffusion coefficient (ADC) map demonstrates a significant reduction of the ADC in the right peripheral zone (*arrow*) with some extension on the left side. This reflects an increased cellular density specific of prostatic tumor
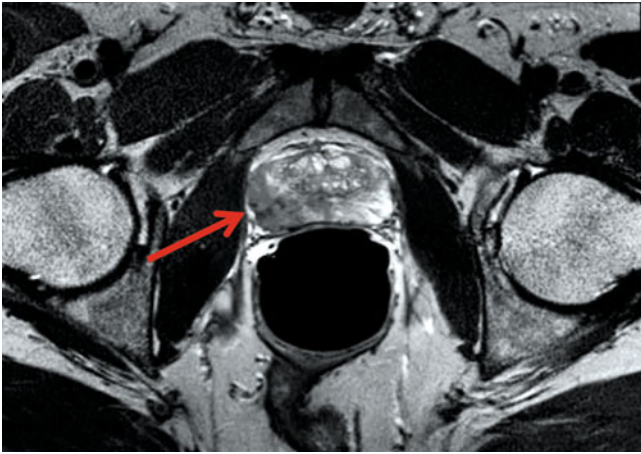
**Fig. 5.21** Large prostatic tumor invading the entire right peripheral zone (*arrow*) with some extension on the left side with a strong hypointensity on T2 images with endorectal coil. On the right size there is a bulging of the capsule associated to some capsule loss reflecting an extra-capsular dissemination
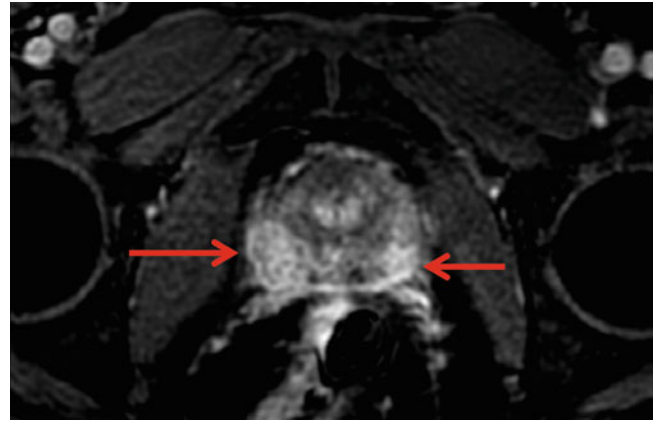


**Fig. 5.22** Perfusion MRI after Gd injection. The right peripheral zone and to some extend also on the left peripheral zone (*arrows*) demonstrate a hypervascularization in the area of T2 hypointensity corresponding to the adenocarcinoma

**Fig. 5.23** Fused PET/MR images showing the localization of the prostatic tumor in the right peripheral zone on T2 3D VISTA as well as positive radiotracer uptake in three abnormal lymph nodes. Note that two of these abnormal lymph nodes measure less than a centimeter in diameter and there would have been classified as benign lymph node
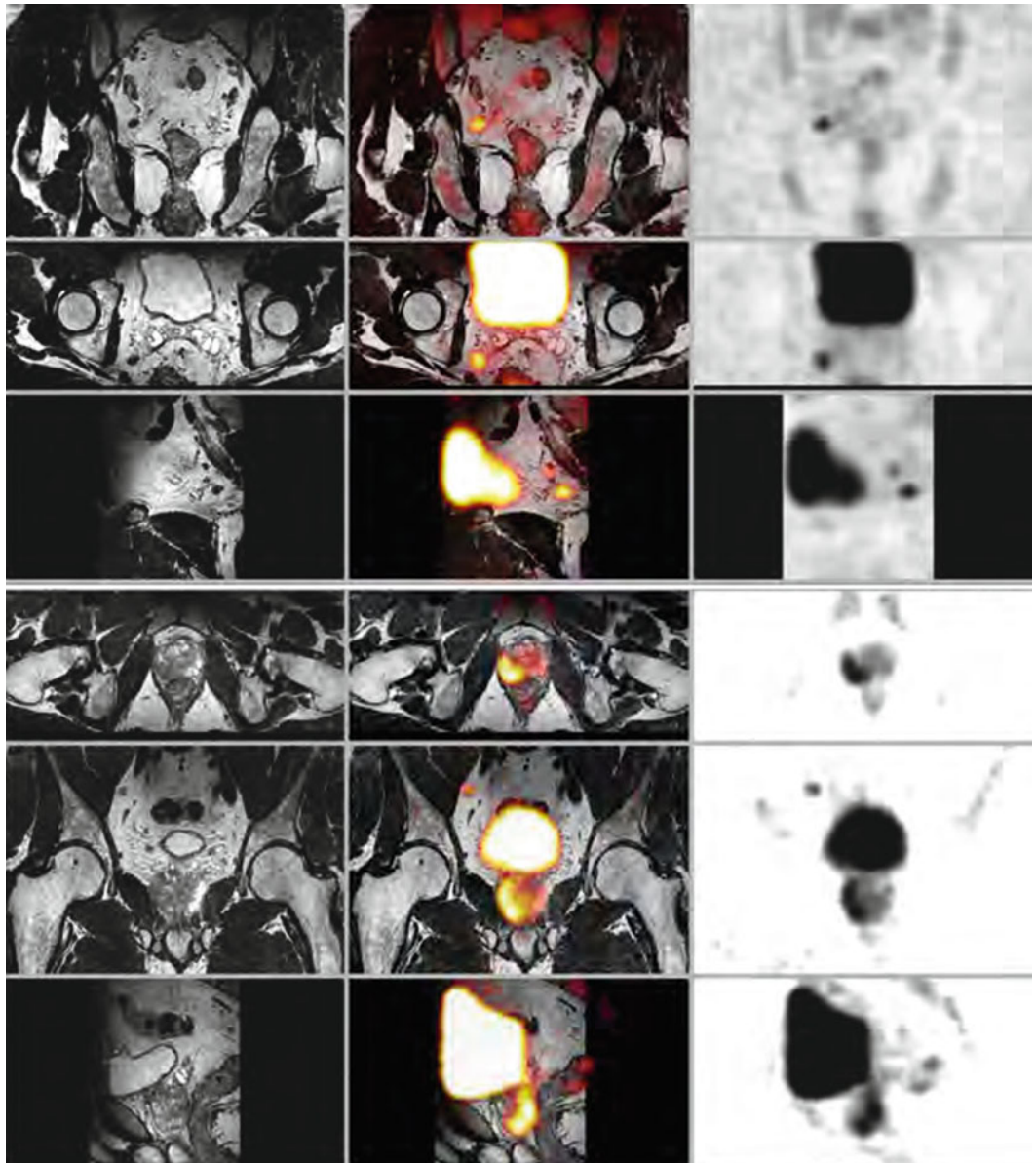
## Multiple Bone Metastases of Prostate Cancer

### Clinical History

Sixty-seven-year-old patient with prostate adeno-carcinoma, Gleason score 5 + 5 and PSA at 5.98 µg/l.

### Imaging Technique

PET: 10 min dynamic acquisition obtained immediately after injection of 240 MBq of F-18 Fluorocholine followed by whole body scan obtained 10 min after injection and a late acquisition centered on the prostate.

MRI: a complete diagnostic MRI study was acquired in the same session including a 2D T2 Fast SE (TR/TE 4,000/120 ms – slice thickness 3 mm – 432×386 for the axial acquisition – FOV 22 cm) with both an endorectal coil and an external 6 array coil, and after removal of the endorectal coil, a 3D T2 fast spin echo MR sequence (3D VISTA) (TR/TE 2,000/243 ms, matrix 392×448/×25, FOV 390 mm and slice thickness 1 mm) and a diffusion SE EPI sequence (TR/TE 3,644/66 ms – slice thickness 3 mm – FOV 200 mm – matrix 88/Å~ 9, 4 b values 0, 500, 1,000, 1,500 s/mm$^2$).

### Findings

Hypermetabolic prostate tumor covering entire left lobe from apex to base and also spreading to the right lobe. Extracapsular invasion is consistent with local invasion covering left neuro-vascular bundle.

PET images showing a hypermetabolic lymph node below the iliac bifurcation with SUV 3.1 and a millimetric hypermetabolic left ilio-obturator lymph with SUV max. 2.1.

Multifocal hypermetabolic bone lesions at the right iliac (SUV max. 3.5), at the left iliac wing (SUV max. 3.7) at the left sacroiliac joint, at the ilio-pubic branch right (SUV max. 7.3), the right ischio-pubic branch (SUV 6.3) and at left ischial tuberosity (SUV max. 5.5) are present.

### Teaching Points

PET/MRI imaging allows a comprehensive staging of remote metastasis by combining the two modalities in a single examination.
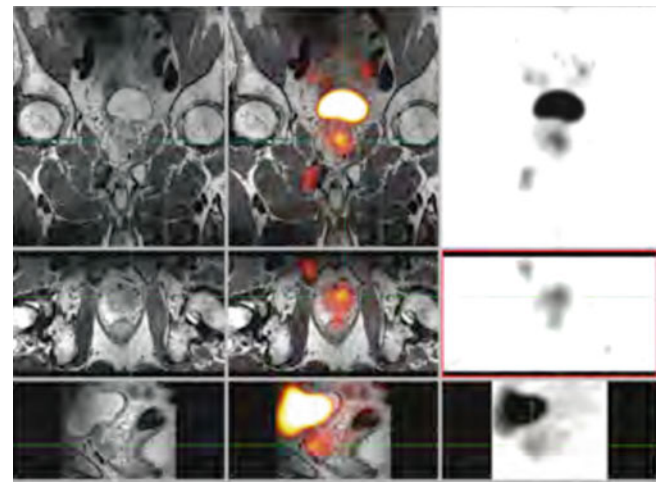


**Fig. 5.24** The large hypermetabolic tumor in two lobes of the prostate also visible in T2 MR images

**Fig. 5.25** eThrive MR image showing the iliac lymph node below the bifurcation with SUV max. of 2.1 (*arrows*)
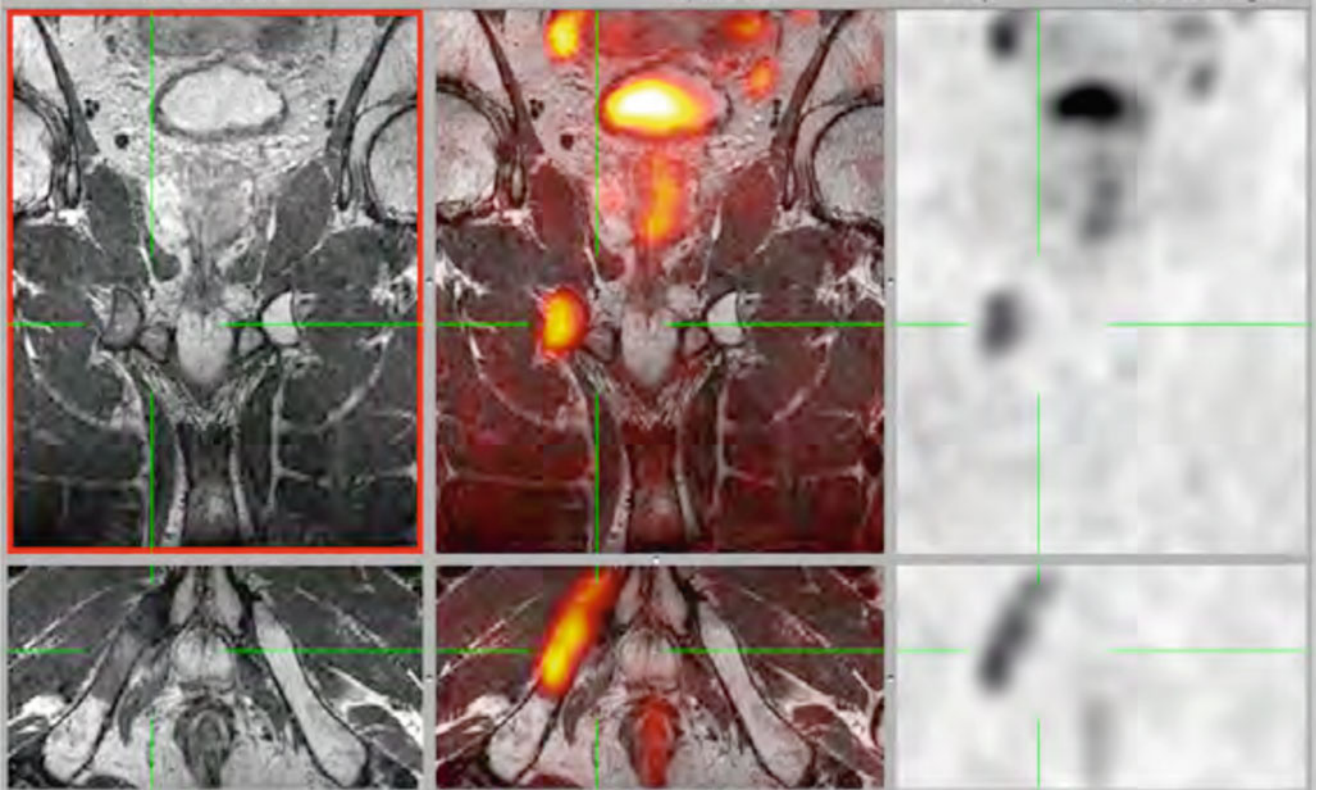
**Fig. 5.26** Coronal (*top*) and axial (*bottom*) PET/MR images of the pelvis showing the metastatic bone lesions of the right iliac branch also clearly visible on T2 weighted 3D VISTA MR images
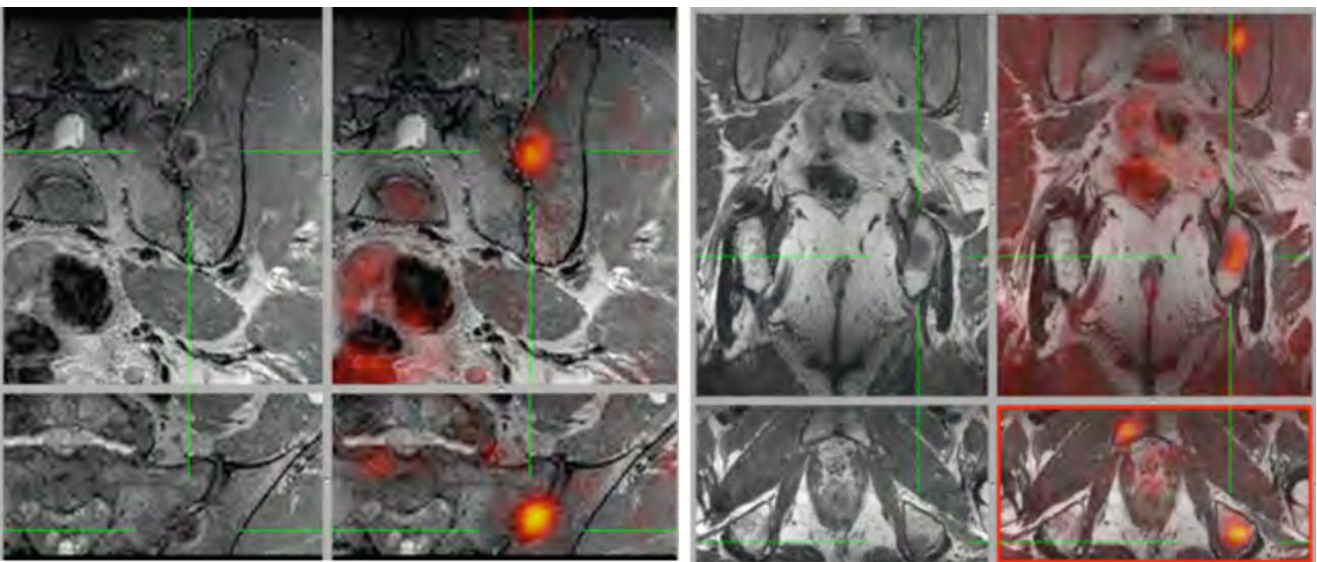


**Fig. 5.27** Coronal (*top*) and axial (*bottom*) PET/MR images of the pelvis showing multiple bone metastases of the left pelvic and iliac bones also visible on T2 weighted 3D VISTA MR images

## Primary Prostate Cancer with Extraprostatic Extension

### Clinical History

Sixty-five-year-old patient presents with an initial PSA-value of 11.2 ng/ml. Endorectal biopsy confirmed prostate cancer (cT3a, Gleason 4+5=9).

### Imaging Technique

Whole body PET/MR images acquired 37 min after iv injection 811 MBq $^{11}$C-Choline, 77 kg.

3 beds × 4 min together with coronal T1w TSE and axial T2w haste fs. 1 bed (pelvis) a 15 min together with ax T2 TSE, ax T1 TSE, ax DWI, ax T1w TWIST CM dynamic. Post gadolinium axial T1w VIBE from chest to pelvis. Head/neck and two body coils.
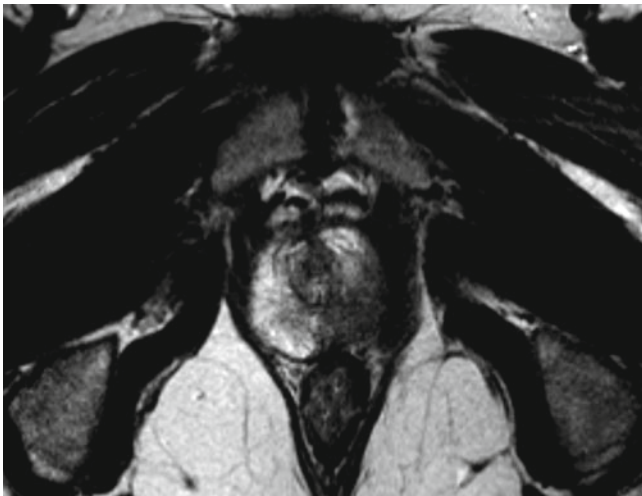


**Fig. 5.28** Axial T2w TSE of prostatic apex shows a relative hypointense signal in the peripheral zone of the *left side* highly suspicious for prostate cancer. The missing delineation of the capsule (compared to the *right side*) raises the suspicion of extracapsular extension

### Findings

T2w TSE sequences are very sensitive in the detection of prostate cancer in the peripheral zone which normally shows a hyperintense signal. Missing delineation of the prostatic capsule is suspicious for extracapsular extension.

### Teaching Points

The superb anatomical delineation of the prostate fossa in MRI allows local staging of prostate cancer. This is a clear advantage of PET/MR compared to PET/CT.
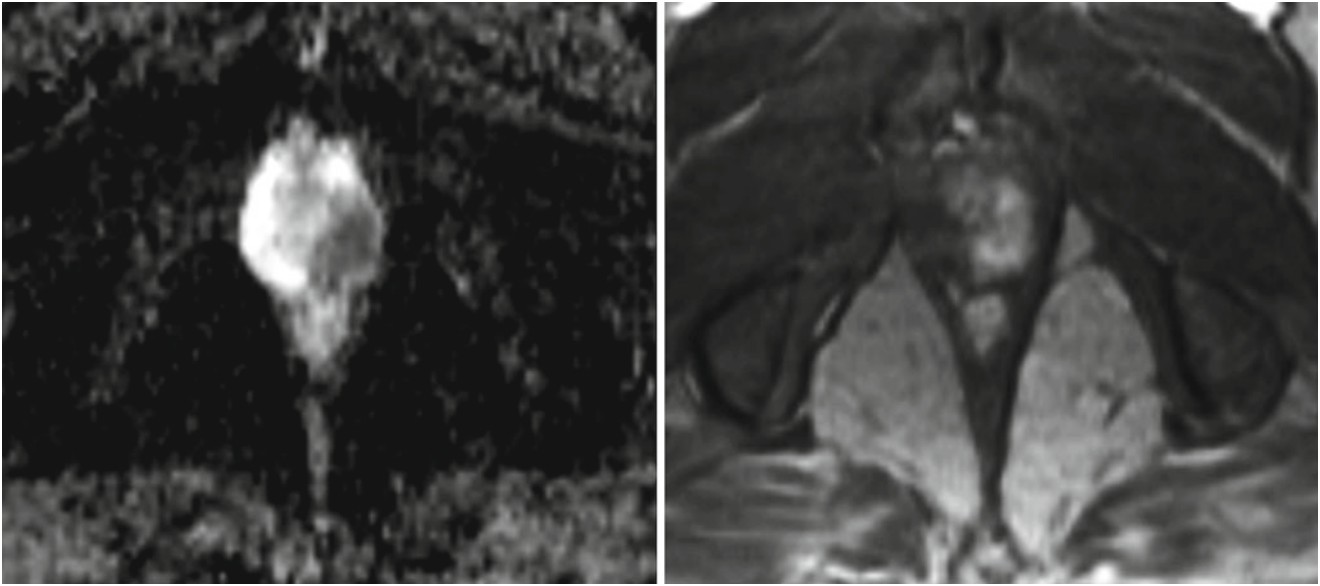
**Fig. 5.29** Axial diffusion weighted imaging (DWI) demonstrate a highly restricted diffusion (low ADC-value) in the left peripheral zone (*left*). An intense and early enhancement of the corresponding region can be found in the arterial phase of the dynamic contrast enhanced MRI sequence (*right*). Both findings support the uspicion of prostate cancer from the T2w TSE sequence



**Fig. 5.30** A high focal uptake in $^{11}$C-Choline PET (*left*) is located exactly in the area of the abnormalities presented by MRI shown in the fused PET/T2w TSE image (*right*)

## Prostate Cancer in the Central Zone

### Clinical History

Seventy-three-year-old patient with a PSA-value of 34 ng/ml suspicious for prostate cancer. No prior endorectal biopsy has been performed.

### Imaging Technique

Whole body PET/MR images acquired 32 min after iv injection 809 MBq $^{11}$C-Choline, 71 kg.

3 beds × 4 min together with coronal T1w TSE and axial T2w haste fs. 1 bed (pelvis) a 15 min together with ax T2 TSE, ax T1 TSE, ax DWI, ax T1w TWIST CM dynamic. Post CM axial T1w VIBE from chest to pelvis. Head/neck and two body coils.

### Findings

T2w sequences show superb anatomical details of the prostate with a hypointense region in the anterior part on the left side. With morphological sequences alone in MRI no definite differentiation between prostate cancer and benign prostatic hyperplasia (BPH) can be made. Functional imaging with diffusion-weighted imaging (DWI) and $^{11}$C-Choline PET confirm the presence of prostate cancer in the anterior portion of the gland.

### Teaching Points

Detection of prostate cancer in the central zone is often unambiguous with morphological MR sequences. However DWI and $^{11}$C-Choline PET can help in the differentiation between BPH and prostate cancer.
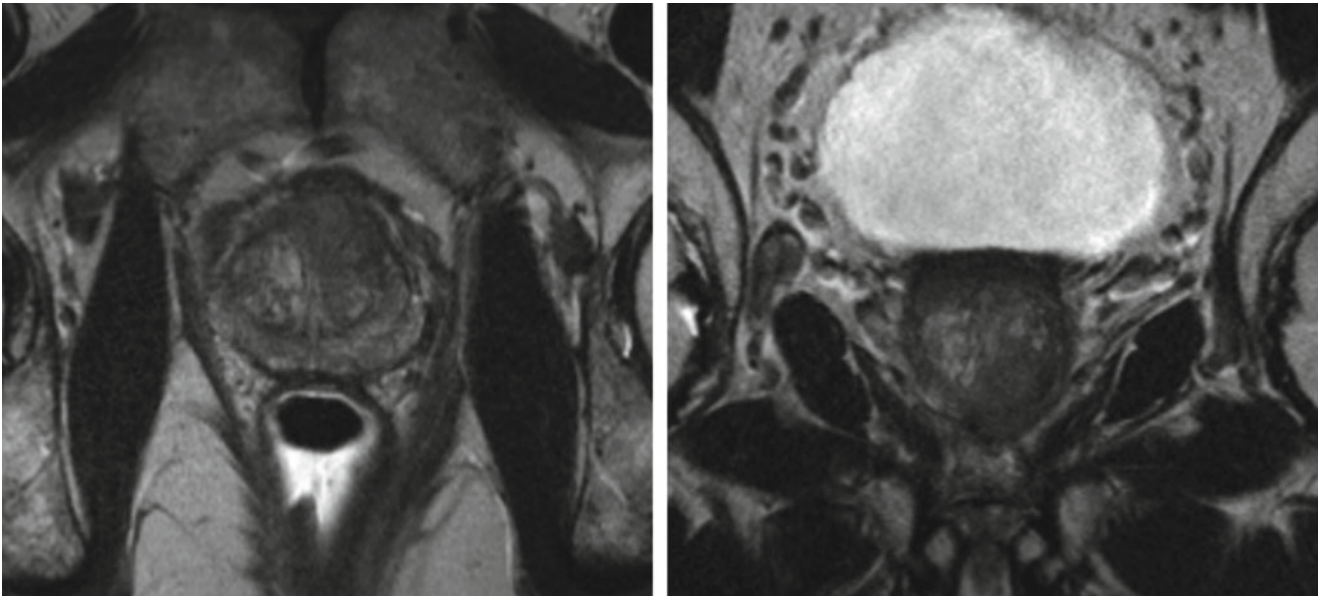


**Fig. 5.31** Morphological T2w TSE sequences in the axial and the coronal plane demonstrate superb anatomical details of the prostate fossa. A hypointense region in the anterior part of the left side is suspicious for prostate cancer. However benign prostatic hyperplasia can have similar appearance on MRI
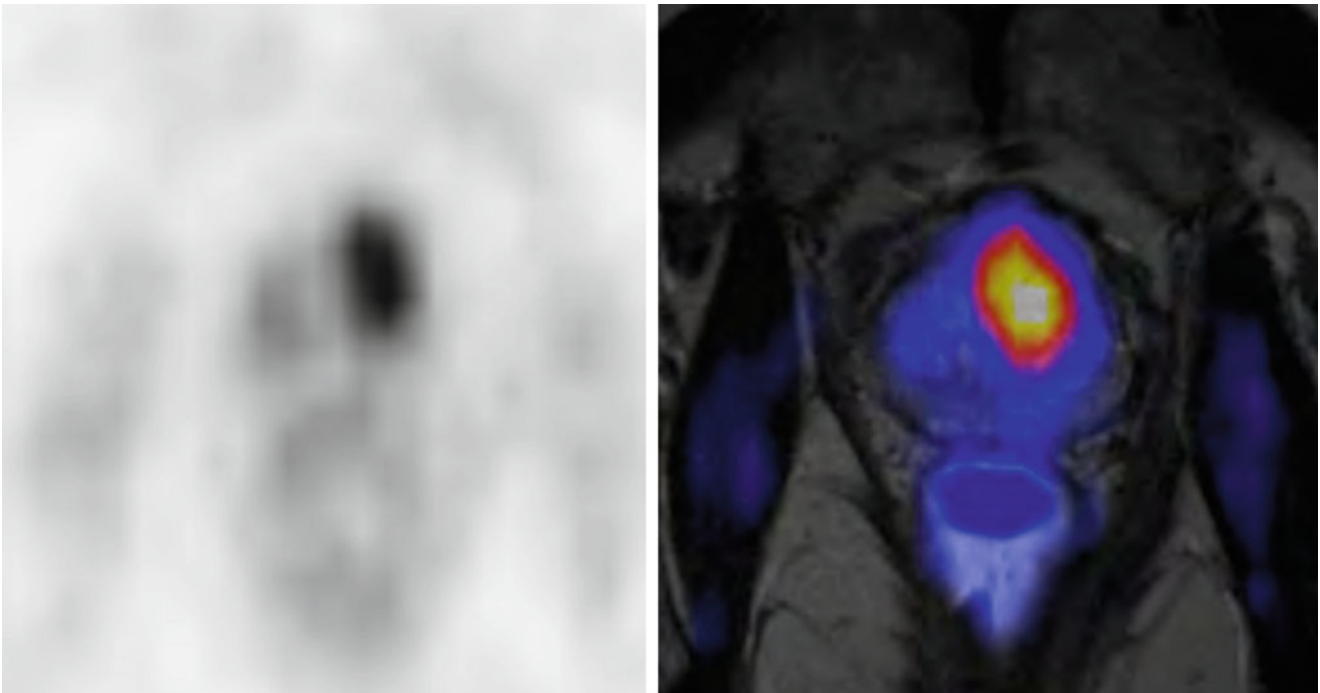
**Fig. 5.32** ^{11}C-Choline PET shows an intense focal uptake in the left anterior part of the prostate highly suspicious for prostate cancer
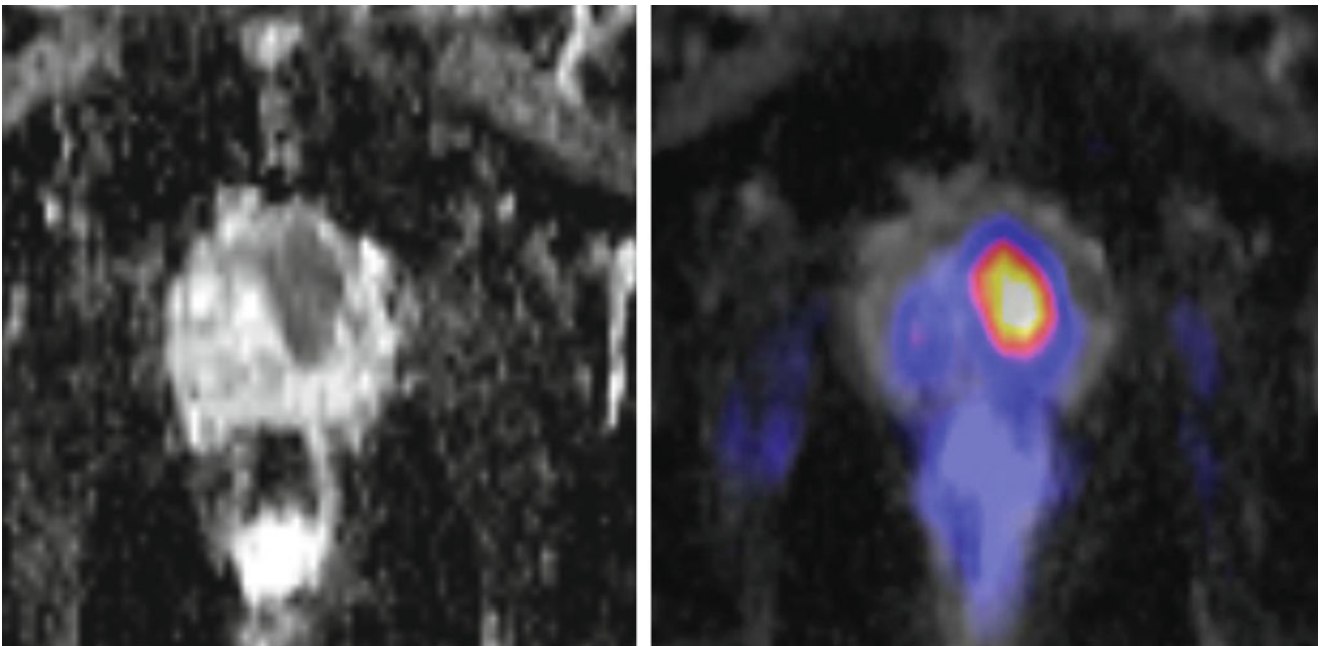


**Fig. 5.33** The parametric ADC (apparent diffusion coefficient) map derived from diffusion-weighted imaging sequences shows an area of highly restricted diffusion (low ADC-value) in the left anterior part of the prostate. In the central zone this can be more specific for prostate cancer than hypointensity in T2w sequences. Fusion with ^{11}C-Choline PET demonstrates a good concordance between the findings in PET and DWI

## Multiparametric Imaging in Primary Prostate Cancer

### Clinical History

Fifty-nine-year-old patient with slowly rising PSA-value over 5 years and a history of negative biopsy 3 years ago. The current PSA-value is 11.3 ng/ml.

### Imaging Technique

Whole body PET/MR images acquired 66 min after iv injection 750 MBq $^{11}$C-Choline, 58 kg.

3 beds × 4 min together with coronal T1w TSE and axial T2w haste fs. 1 bed (pelvis) a 15 min together with ax T2 TSE, ax T1 TSE, ax DWI, ax T1w TWIST CM dynamic. Post CM axial T1w VIBE from chest to pelvis. Head/neck and two body coils.

### Findings

A T2w-hypointense lesion in the peripheral zone of the left side is highly suspicious for primary prostate cancer. In addition focal increased uptake in PET, restricted diffusion in DWI, high wash-in DCE-MRI and a pathological choline peak in MRS are indicative of primary prostate cancer.

### Teaching Points

Multiparametric PET/MR imaging of primary prostate cancer can further increase tumor detection and possibly guide biopsy especially in patients with prior negative histopathology.
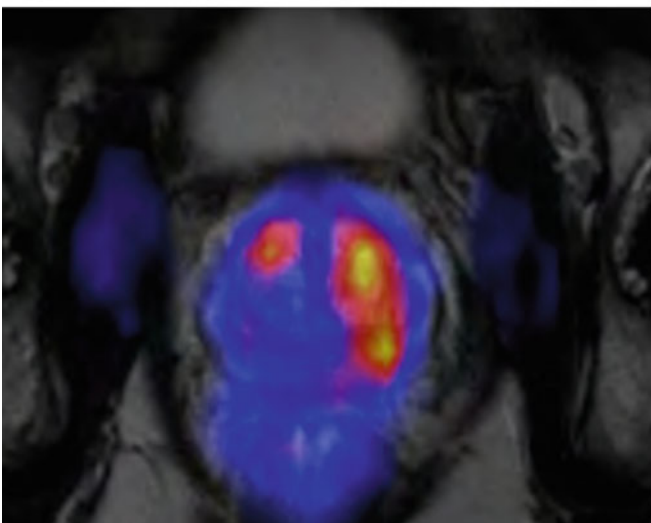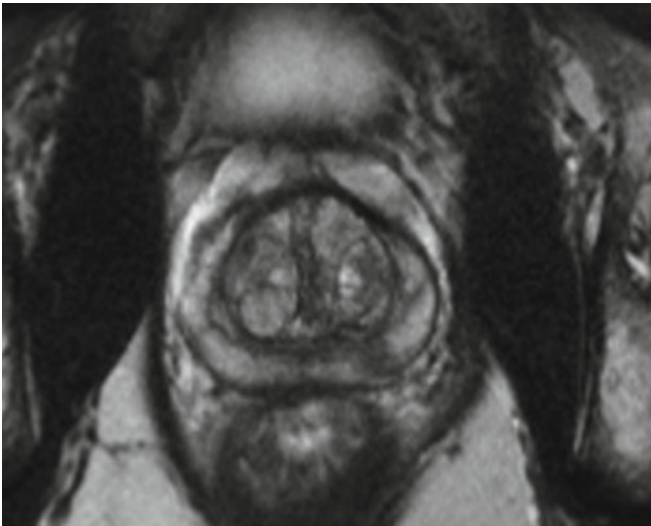


**Fig. 5.34** The axial T2w TSE sequence shows a hypointense lesion in the peripheral zone on the left side which is highly suspicious for primary prostate cancer (*left top*). Diffuse partially focal uptake is demonstrated in the central zone with a focus of high uptake in the left peripheral zone (*right top*). Fused PET/T2w image documents a good correlation of the abnormal findings in the left peripheral zone (*bottom*)
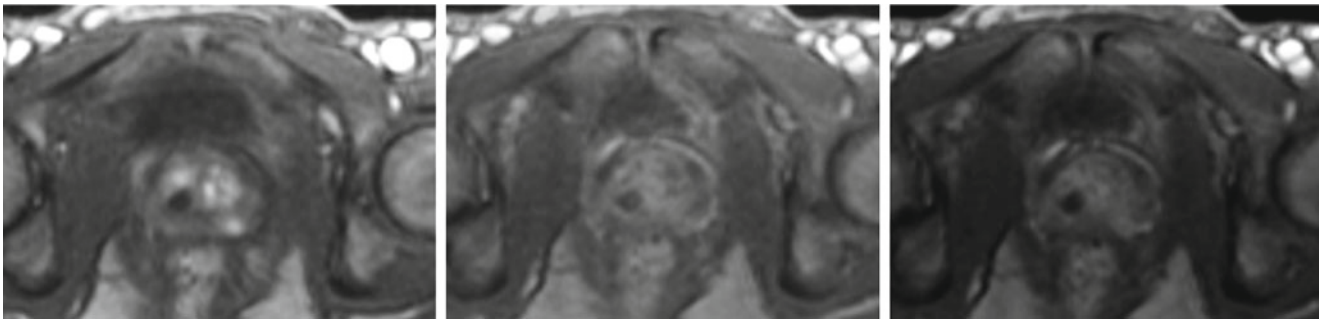
**Fig. 5.35** Dynamic contrast enhancement (DCE) MRI of the prostate gland. Arterial phase (*left*) shows an early enhancement in the left peripheral zone suspicious for primary prostate cancer and a diffuse inhomogeneous enhancement in the central zone typical for BPH. In the later phases (*center* and *right*) an inhomogeneous enhancement is found in the whole prostate nearly completely obscuring the lesion in the peripheral zone
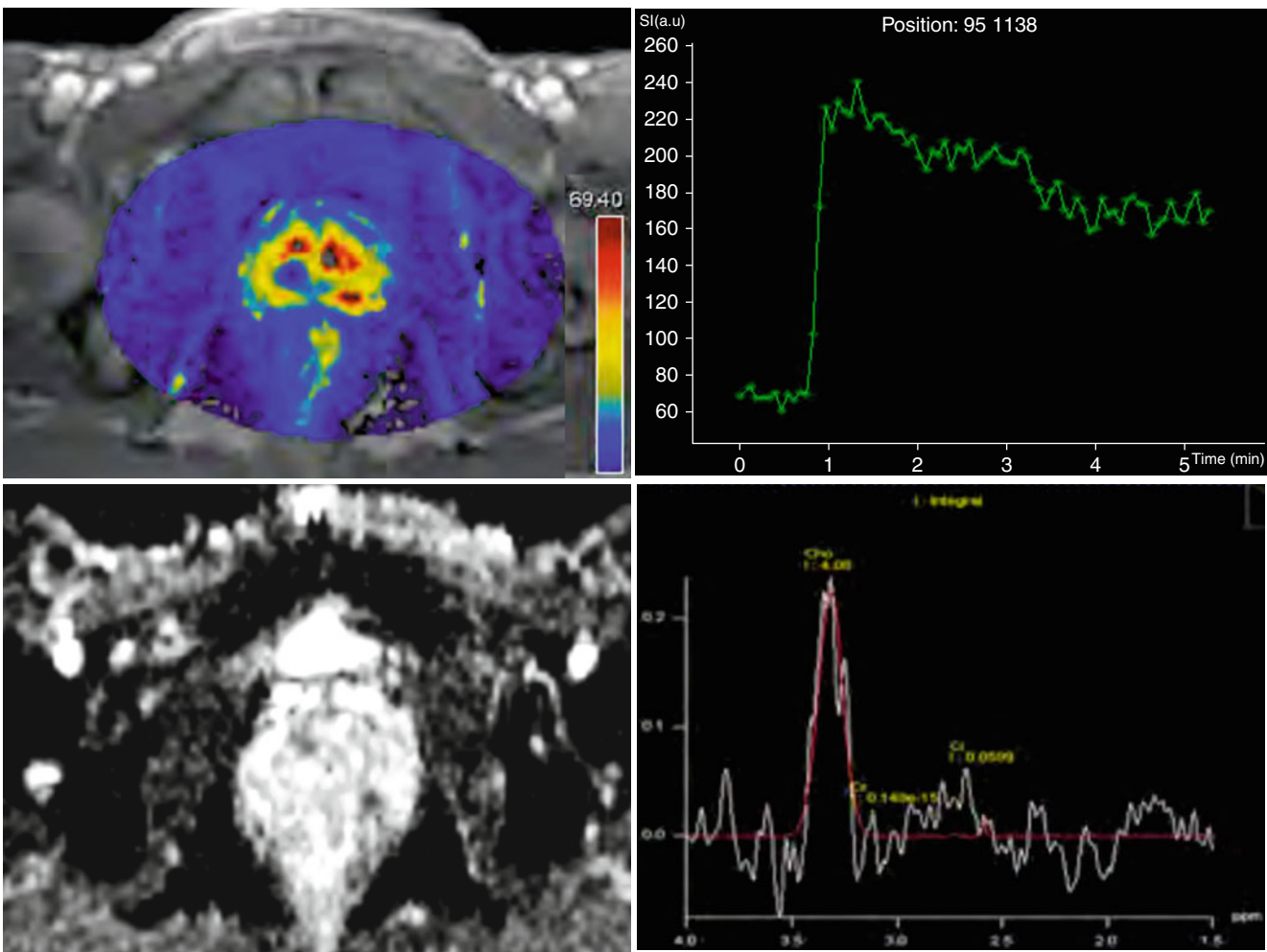


**Fig. 5.36** Parametric map of the DCE-images show an increased AUC (area under the *curve*) in the left peripheral zone (*left top*). ROI analysis demonstrates an early wash-in as well as an wash-out typical for a malignant lesion (*top right*). Restricted diffusion with a low ADC-value can be found in this region in DWI-MRI (*bottom left*). MR-spectroscopy reveals a high peak of choline

## Recurrence After Brachytherapy

### Clinical History

Seventy-two-year-old patient presenting with rising PSA (10.6 ng/ml) 2 years after brachytherapy.

### Imaging Technique

Whole body PET/MR images acquired 46 min after iv injection 883 MBq ^{11}C-Choline, 86 kg.

4 beds × 4 min together with coronal T1w TSE and axial T2w haste fs. 1 bed (pelvis) a 15 min together with ax T2 TSE, ax DWI, ax T1w TWIST CM dynamic. Post CM axial T1w VIBE from chest to pelvis. Head/neck and two body coils.

### Findings

A high focal uptake of ^{11}C-Choline in PET strongly indicates local recurrence. MRI is impaired due to metal artifacts from the implanted seeds. However it demonstrates a relative sparing of the seeds in the zone with the recurrent tumor.

### Teaching Points

The metallic seeds from Brachytherapy create susceptibility artifacts in MRI. In these cases information from PET can become crucial for detection of local recurrence.
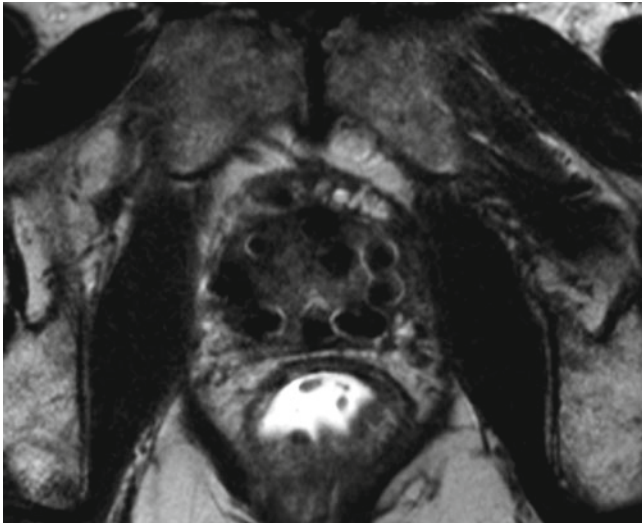


**Fig. 5.37** Usually in MRI of the prostate gland a T2w sequence with small field-of-views serves for anatomical delineation of the prostate gland and enables detection of prostate cancer especially in the peripheral zone. Hence after Brachytherapy image quality is impaired
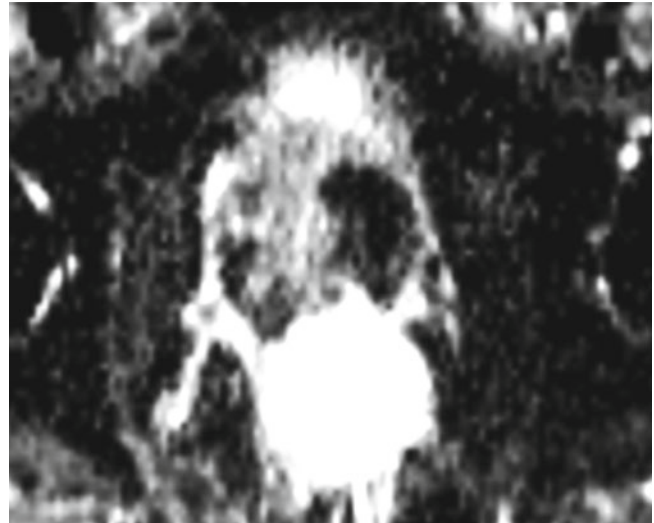


**Fig. 5.38** Modern imaging techniques like DWI (diffusion weighted imaging) enable higher detection rates of recurrent local prostate cancer. However the use is hampered by implanted metal

**Fig. 5.39** In the T1w VIBE GRE-sequence intense susceptibility artifacts demonstrate the location of the seeds with a relative sparing of the right anterior part of the prostate
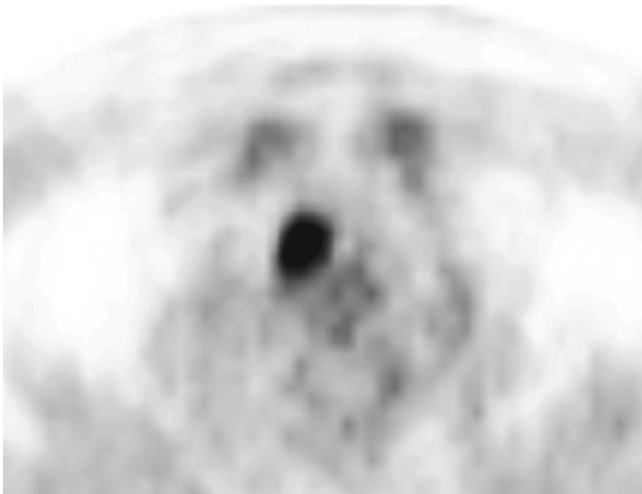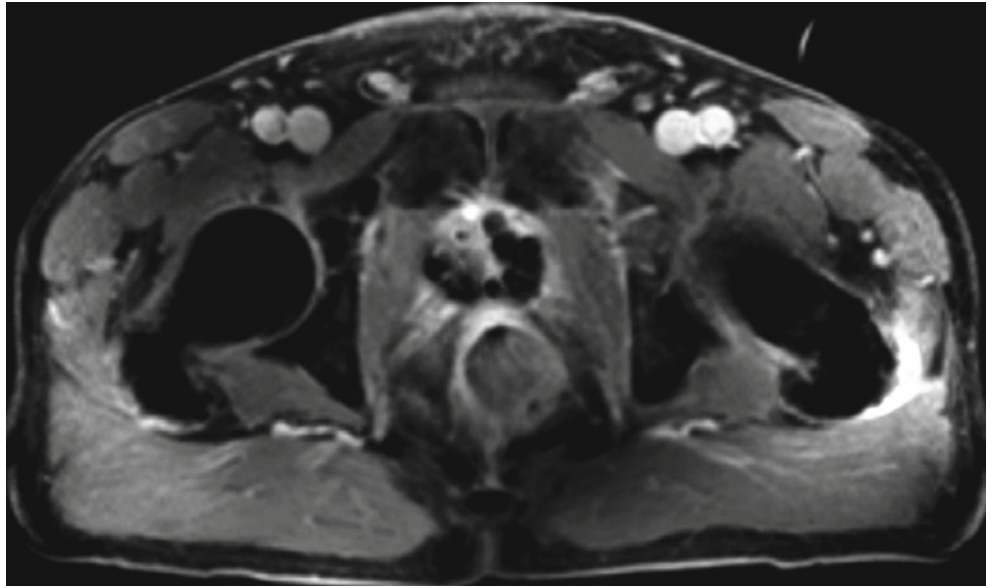




**Fig. 5.40** High focal uptake of ^{11}C-Choline in PET indicates local recurrence/remaining tumor
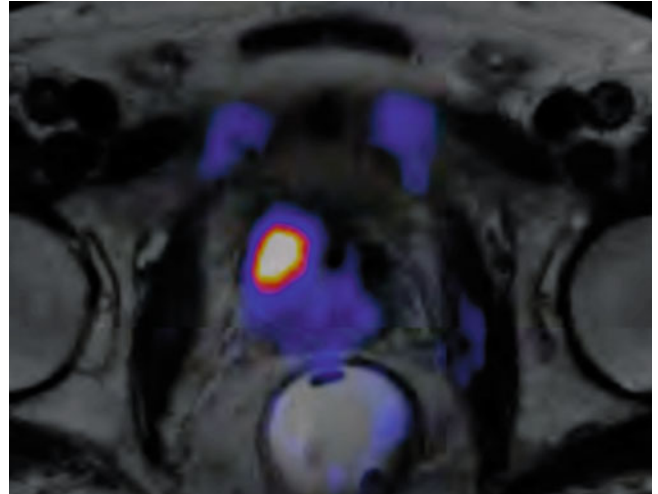


**Fig. 5.41** Fusion from PET and T2w demonstrates the exact anatomical location of the local recurrence

## Lymph Node Metastasis from Recurrent Prostate Cancer

### Clinical History

Seventy-one-year-old patient presenting with rising PSA (34.5 ng/ml) 3 years after radiation therapy of the prostate.

### Imaging Technique

Whole body PET/MR images acquired 56 min after iv injection 770 MBq $^{11}$C-Choline, 74 kg.

4 beds × 4 min together with coronal T1w TSE and axial T2w haste fs. 1 bed (pelvis) a 15 min together with ax T2 TSE, ax DWI, ax T1w TWIST CM dynamic. Post CM axial T1w VIBE from chest to pelvis. Head/neck and two body coils.

### Findings

A pararectal lymph node which is slightly enlarged and rounded appears suspicious in morphological imaging. Highly restricted diffusion and high uptake of $^{11}$C-Cholin confirm the malignant nature.

### Teaching Points

This case demonstrates the additional value of multi-parametric PET/MR compared to PET/CT. Besides the functional information from PET, PET/MR can also provide molecular information from MRI – in this case the restricted diffusion in a malignant lymph node in prostate cancer.
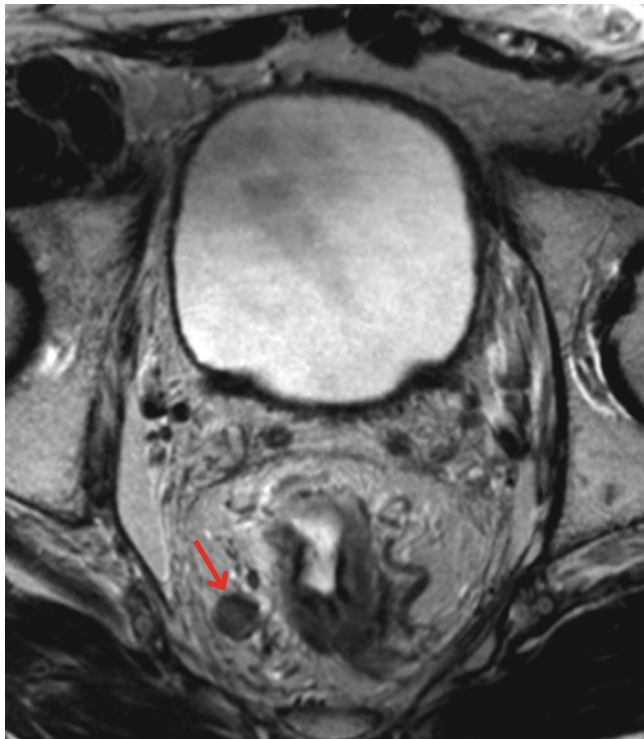


**Fig. 5.42** Anatomical T2w TSE demonstrate an enlarged lymph node in the mesorectal fascia which is an untypical location for a lymph node metastases in prostate cancer (*arrow*)
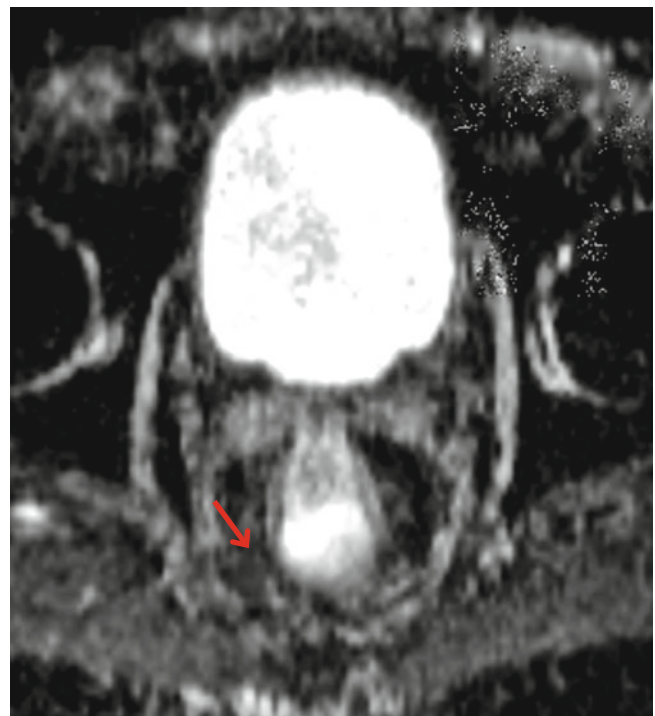


**Fig. 5.43** The ADC (apparent diffusion coefficient) – map of DWI shows highly restricted diffusion in the suspicious lymph node (*arrow*)

**Fig. 5.44** Coronal T1w TSE demonstrates the whole field-of-view from PET/MR and also outlines the lymph node in the mesorectal fat
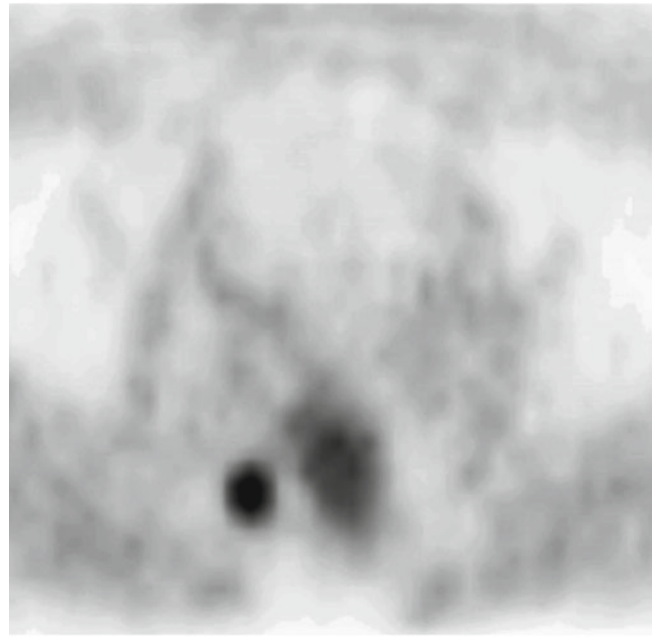


**Fig. 5.45** High uptake of $^{11}$C-Choline in a morphologically enlarged lymph node can be regarded as diagnostic for a metastases in the case of PSA-recurrent prostate cancer
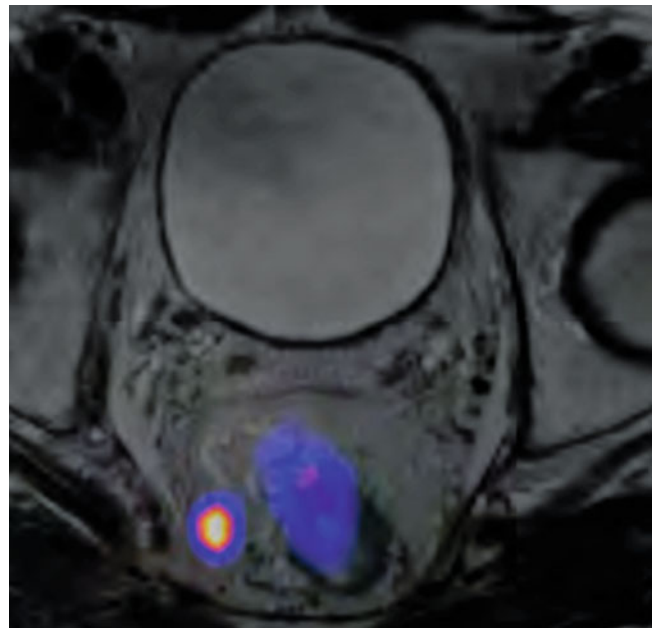


**Fig. 5.46** Fusion of PET and T2w TSE shows a perfect anatomical coregistration of the focal increased uptake in PET and the suspicious lymph node

## Bone Metastases in Prostate Cancer After Radiotherapy

### Clinical History

Eighty-five-year-old patient status post radical prostatectomy 8 years ago. He presents with rising PSA (25.9 ng/ml) despite radiation of multiple bone metastases in the last 2 years.

### Imaging Technique

Whole body PET/MR images acquired 53 min after iv injection 850 MBq $^{11}$C-Choline, 70 kg.

4 beds × 4 min together with coronal T1w TSE and axial T2w haste fs. 1 bed (pelvis) a 15 min together with ax T2 TSE, ax DWI, ax T1w TWIST CM dynamic. Post CM axial T1w VIBE from chest to pelvis. Head/neck and two body coils.

### Findings

In this patient with prior radiotherapy T1w SE sequences show the conversion to fatty bone marrow in the whole spine. Additional T1w hypointense areas with high uptake of $^{11}$C-Choline indicate new/residual bone metastases which now could be treated with focused radiation therapy.

### Teaching Points

MRI with T1w SE sequences is superior to CT in outlining the anatomical extent of bone metastases. Therefore it can serve for a more exact planning of radiation therapy especially in patient who underwent prior radiotherapy.
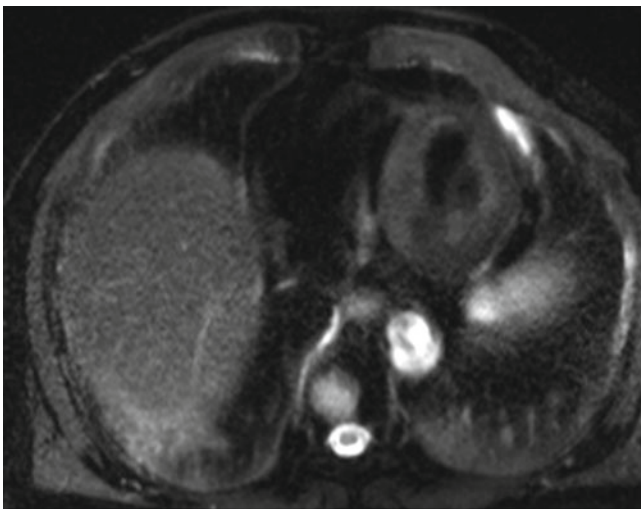


**Fig. 5.47** The axial T2w fs sequence shows a round hyperintense area in the thoracic spine. T2w hyperintensity of a bone metastasis usually indicates viable tumor tissue compared to T2w hypointensity which is a sign of prior effective treatment (esp. by radiation therapy)
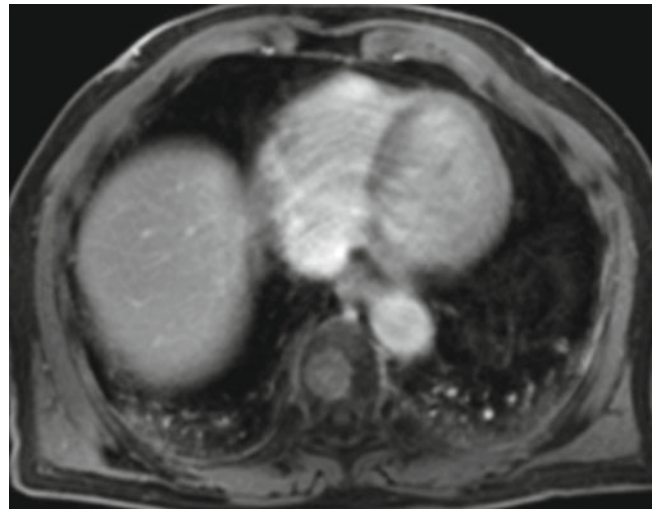


**Fig. 5.48** Axial post contrast VIBE sequence with fat saturation shows a moderate contrast enhancement of the lesion
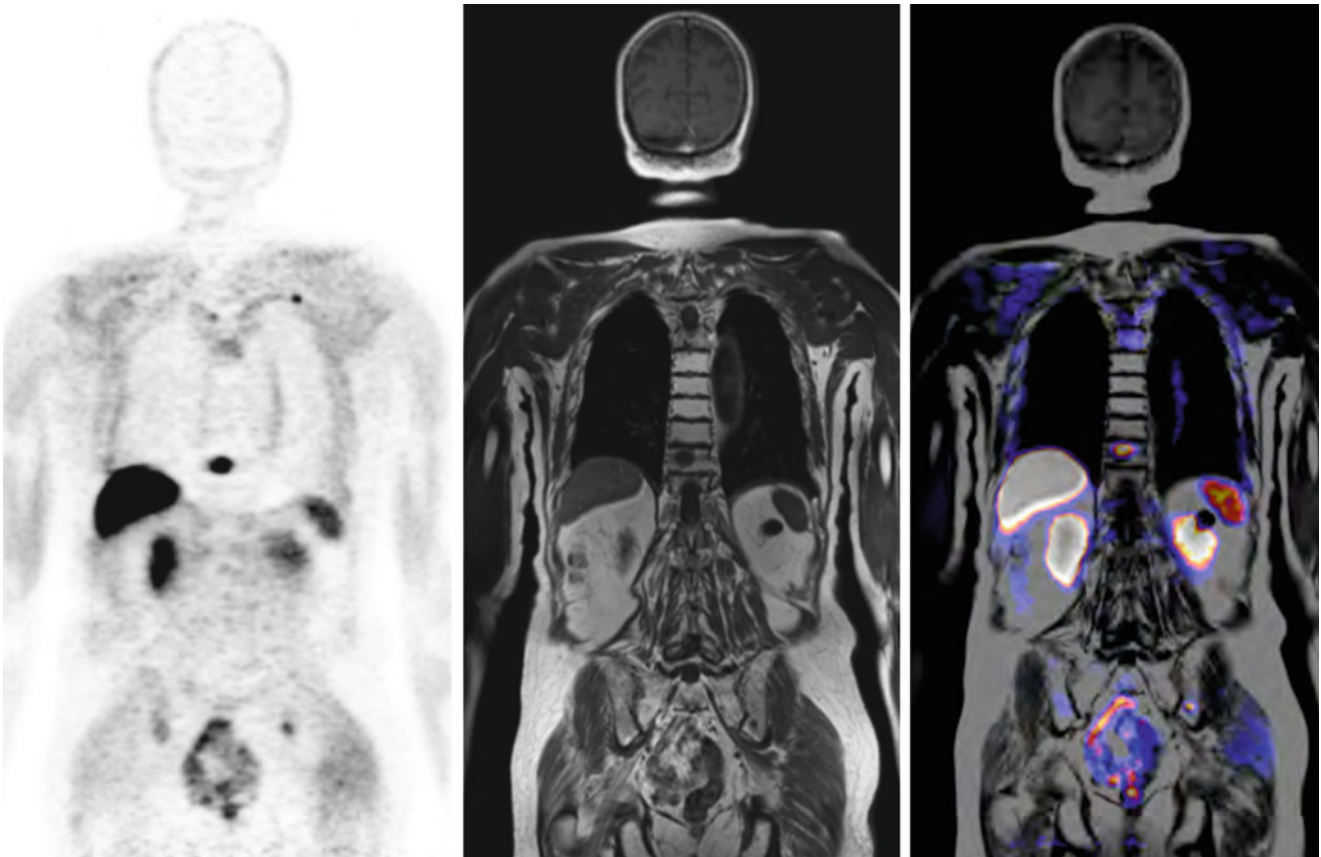
**Fig. 5.49** Coronal images show the extent of bone metastases in this patient. PET demonstrates the highest uptake of $^{11}$C-Choline in a lesion of the lower thoracic spine. Other lesions are located in the left pelvis and the ribs (*left*). T1w TSE show fatty conversion of the bone marrow indicating prior radiation therapy and hypointense lesions corresponding with the high uptake in PET (*middle*). Fused T1w TSE and PET demonstrate good correlation between the uptake in PET and the hypointense lesions in MRI

## Discrimination of Viable and Effectively Treated Bone Metastases

### Clinical History

Sixty-year-old patient after with increasing PSA over 2 years (21.5 ng/ml) after radical prostatectomy and prior radiation of the right pelvis due to a single bone metastases.

### Imaging Technique

Whole body PET/MR images acquired 42 min after iv injection 764 MBq $^{11}$C-Choline, 75 kg.

3 beds × 4 min together with coronal T1w TSE and axial T2w haste fs. 1 bed (pelvis) a 15 min together with ax T2 TSE, ax DWI, ax T1w TWIST CM dynamic. Post CM axial T1w VIBE from chest to pelvis. Head/neck and two body coils.

### Findings

The patients presents with a treated bone metastasis in the right pelvis which shows no uptake of $11_C$-Cholin and only faint contrast enhancement. In contrast, a new bone metastasis in the sternum has a high uptake in PET as well as an intense contrast enhancement in MRI.

> ### Teaching Points
>
> In contrast to CT, MRI can give additional information about the viability of bone metastases in prostate cancer complementing the information provided by PET.
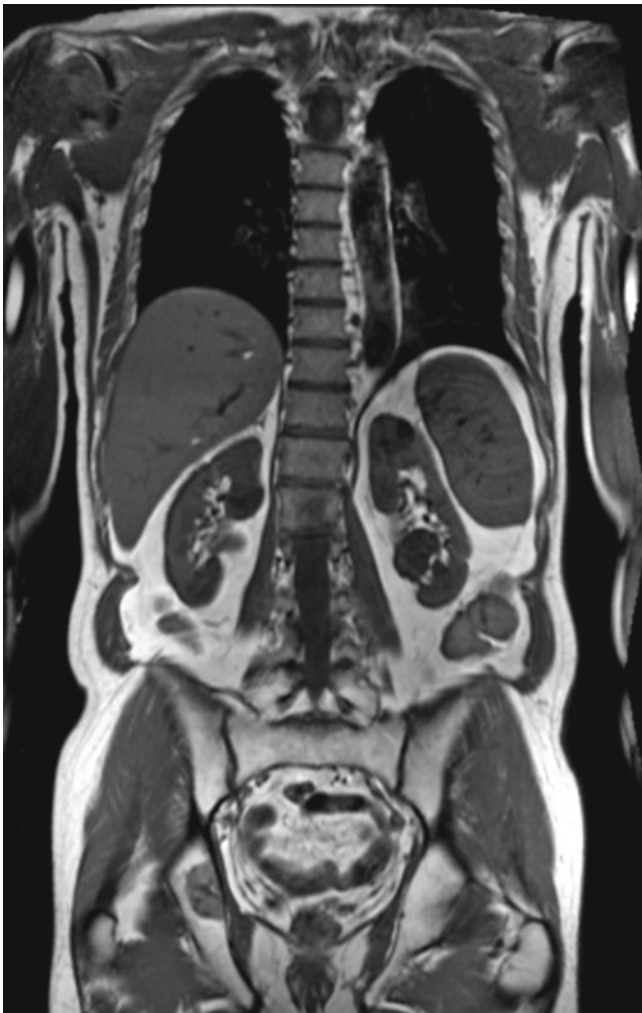


**Fig. 5.50** Coronal T1w TSE shows a hypointense lesion in the right pelvis. T1w alone does not allow to discriminate between active or effectively treated bone lesions
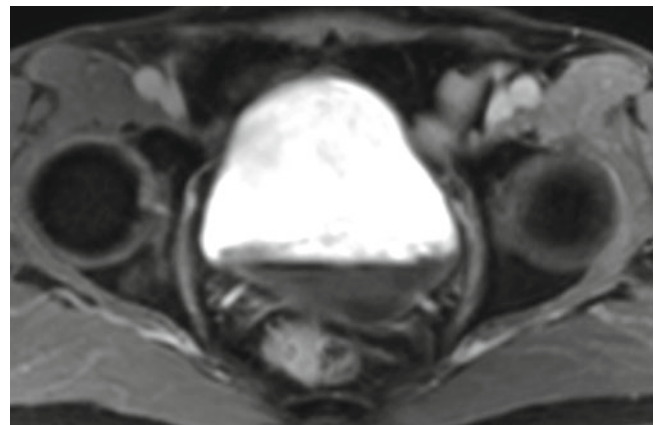


**Fig. 5.51** Axial T1w VIBE fs after contrast media show only faint enhancement of a bone lesion in the right pelvis suggesting effective treatment
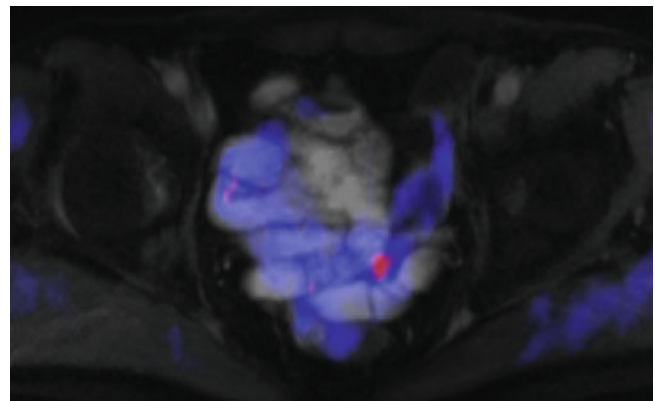


**Fig. 5.52** In axial PET/MR no uptake is noted in the region of the right pelvis
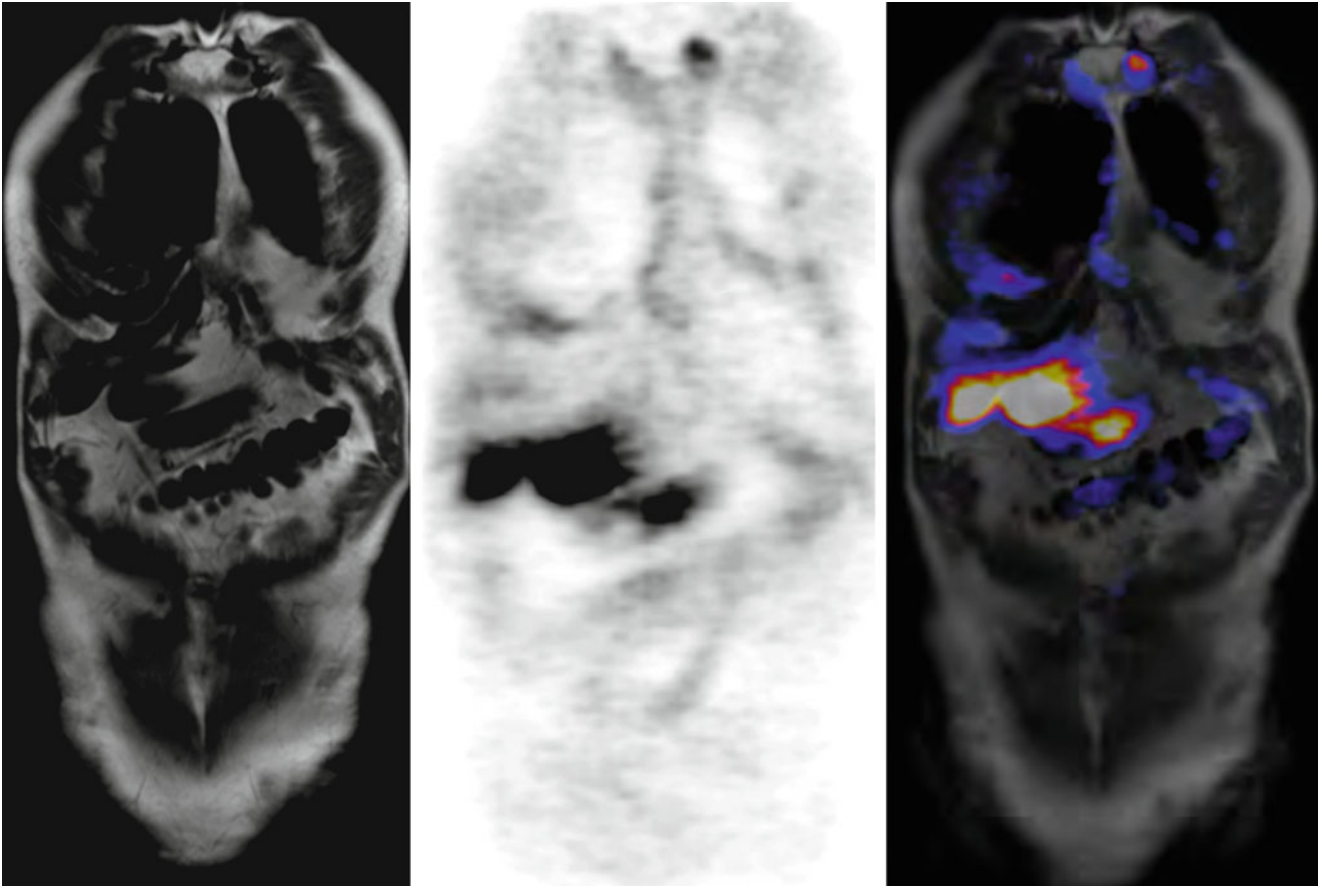
**Fig. 5.53** Coronal PET and T1w TSE show a lesion in the proximal sternum with T1w hypointensity in MRI and high Choline metabolism in PET
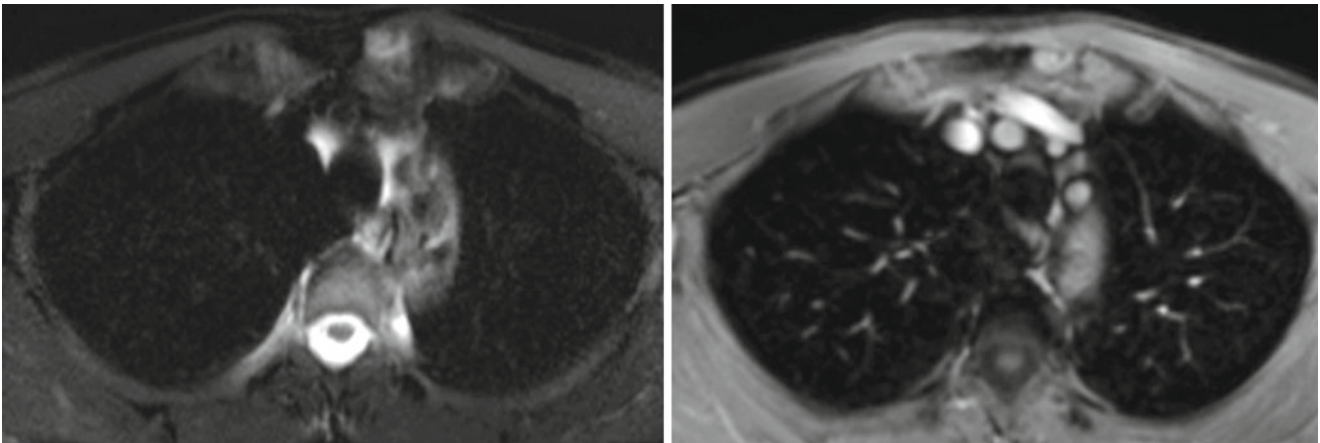


**Fig. 5.54** Axial T2w HASTE fs shows relative hyperintensity of the lesion in the sternum (*left*). In addition T1w VIBE fs after contrast media demonstrates an intense enhancement (*right*). Both findings are indicating a viable bone metastases

## Local Recurrence After Radical Prostatectomy

### Clinical History

Seventy-one-year-old patient presenting with a slow increase of PSA-value from 0.07 ng/ml (nadir) after radical prostatectomy 5 years ago to a current value of 0.31 ng/ml.

### Imaging Technique

Whole body PET/MR images acquired 43 min after iv injection 798 MBq ^{11}C-Choline, 102 kg.

3 beds × 4 min together with coronal T1w TSE and axial T2w haste fs. 1 bed (pelvis) a 15 min together with ax T2 TSE, ax DWI, ax T1w TWIST CM dynamic. Post CM axial T1w VIBE from chest to pelvis. Head/neck and two body coils.

### Findings

PET demonstrates a moderate uptake of ^{11}C-Choline in the area of the former prostate gland. Dynamic contrast enhanced MRI shows an arterial hypervascularisation in the corresponding region.

### Teaching Points

Especially in cases with low PSA-value PET and MRI can provide complimentary information. Hereby accumulating evidence for a possible local recurrence increases the certainty in reporting these findings.
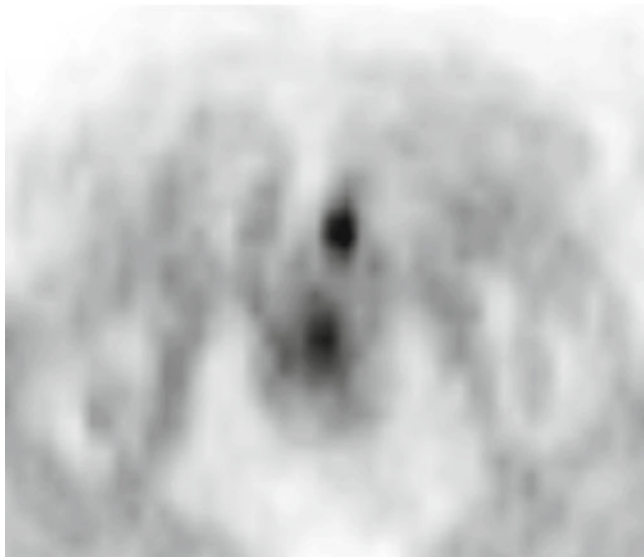


**Fig. 5.55** Moderate uptake of ^{11}C-Choline in the pelvis is suspicious for local recurrence
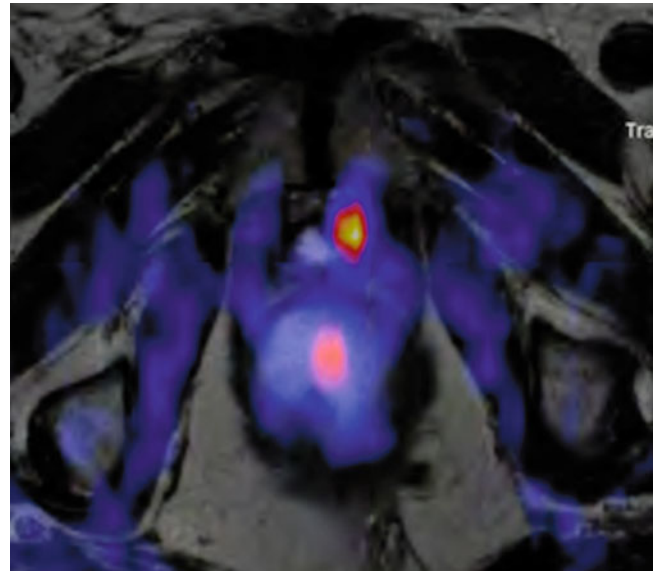


**Fig. 5.56** Axial fused imagines show that the uptake in PET is located at the base of the bladder in the region of the former prostate gland

**Fig. 5.57** High resolution T2w provides superb anatomical resolution with high soft tissue contrast in the pelvis. A slight asymmetry is found at the base of the bladder (*arrow*)
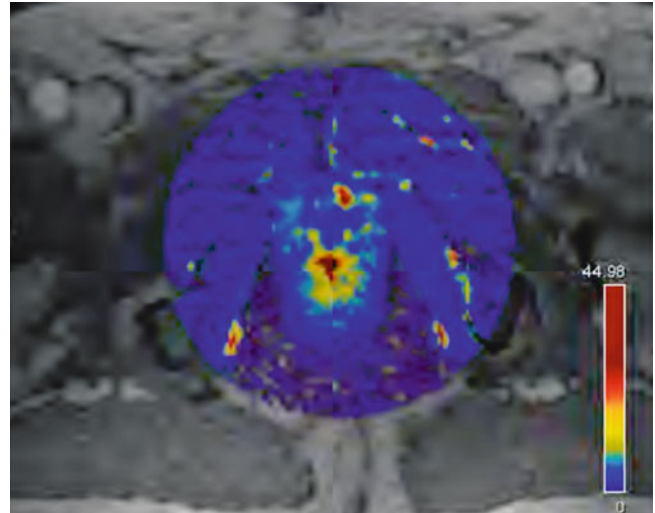


**Fig. 5.59** A parametric map illustrating the influx of contrast media in the first 60s (iAUC60) demonstrates this finding more clearly
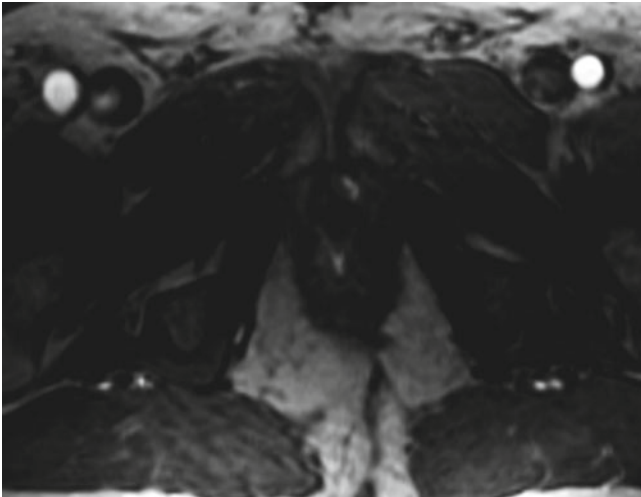


**Fig. 5.58** Axial dynamic contrast enhanced T1 TWIST show a hyper-vascularized region at the base of the bladder corresponding with the uptake in PET

# References

1. Boyle P, Ferlay J (2005) Cancer incidence and mortality in Europe 2004. Ann Oncol 16(3):481–488

2. Carrol CL, Sommer FG, McNeal JE, Stamey TA (1987) The abnormal prostate; MR imaging at 1.5 T with histopathologic correlation. Radiology 163:521–525

3. Turkbey B, Albert PS, Kurdziel K, Choyke PL (2009) Imaging localized prostate cancer: current approaches and new developments. AJR Am J Roentgenol 192:1471–1480

4. Liu IJ, Zafar MB, Lai YH, Segall GM, Terris MK (2001) Fluorodeoxyglucose positron emission tomography studies in diagnosis and staging of clinically organ-confined prostate cancer. Urology 57:108–111

5. Hofer C, Laubenbacher C, Block T, Breul J, Hartung R, Schwaiger M (1999) Fluorine-18-fluorodeoxyglucose positron emission tomography is useless for the detection of local recurrence after radical prostatectomy. Eur Urol 36:31–35

6. Takahashi N, Inoue T, Lee J, Yamaguchi T, Shizukuishi K (2007) The roles of PET and PET/CT in the diagnosis and management of prostate cancer. Oncology 72:226–233

7. Schöder H, Larson SM (2004) Positron emission tomography for prostate, bladder, and renal cancer. Semin Nucl Med 34:274–292

8. Scher B, Seitz M, Albinger W et al (2007) Value of ¹¹C-choline PET and PET/CT in patients with suspected prostate cancer. Eur J Nucl Med Mol Imaging 34:45–53

9. Picchio M, Crivellaro C, Giovacchini G, Gianolli L, Messa C (2009) PET/CT for treatment planning in prostate cancer. Q J Nucl Med Mol Imaging 53:245–268

10. Picchio M, Briganti A, Fanti S et al (2011) The role of choline positron emission tomography/computed tomography in the management of patients with prostate-specific antigen progression after radical treatment of prostate cancer. Eur Urol 59:51–60

11. Castellucci P, Fuccio C, Rubello D et al (2011) Is there a role for ¹¹C-choline PET/CT in the early detection of metastatic disease in surgically treated prostate cancer patients with a mild PSA increase <1.5 ng/ml? Eur J Nucl Med Mol Imaging 38:55–63

12. Jadvar H, Gurbuz A, Li X et al (2008) Choline autoradiography of human prostate cancer xenograft: effect of castration. Mol Imaging 7:147–152

13. Kotzerke J, Prang J, Neumaier B et al (2000) Experience with carbon-11 choline positron emission tomography in prostate carcinoma. Eur J Nucl Med 27:1415–1419

14. De Jong IJ, Pruim J, Elsinga PH et al (2003) 11C-choline positron emission tomography for the evaluation after treatment of localized prostate cancer. Eur Urol 44:38–38

15. Reske SN (2008) [11C]choline uptake with PET/CT for the initial diagnosis of prostate cancer: relation to PSA levels, tumor stage and anti-androgenic therapy. Eur J Nucl Med Mol Imaging 35:1740–1741

16. Reske SN, Blumstein NM, Glatting G (2008) [11C]choline PET/CT imaging in occult local relapse of prostate cancer after radical prostatectomy. Eur J Nucl Med Mol Imaging 35:9–17

17. Hara T, Bansal A, DeGrado TR (2006) Effect of hypoxia on the uptake of [methyl-3H] choline, [1-14C]acetate and [18F]FDG in cultured prostate cancer cells. Nucl Med Biol 33:977–984

18. Breeuwsma AJ, Pruim J, Jongen MM et al (2005) In vivo uptake of [11C]choline does not correlate with cell proliferation in human prostate cancer. Eur J Nucl Med Mol Imaging 32:668–673

19. Pichler BJ, Judenhofer MS, Pfannenberg C. Multimodal imaging approaches: PET/CT and PET/MRI. Handb Exp Pharmacol 2008: 109–132.

20. Boss A, Bisdas S, Kolb A et al (2010) Hybrid PET/MRI of intracranial masses: initial experiences and comparison to PET/CT. J Nucl Med 51:1198–1205